A Linear Regression of Differential PWV Calibration Model to Improve the Accuracy of MODIS NIR All-Weather PWV Products Based on Ground-Based GPS PWV Data

Jiafei Xu and Zhizhao Liu, *Member, IEEE*

***Abstract*—Precipitable water vapor (PWV) products derived from the near-infrared (NIR) channels of the Moderate Resolution Imaging Spectroradiometer (MODIS) instruments, onboard Aqua and Terra satellites, were calibrated using a linear differential PWV (LinearDP) calibration model based on GPS-retrieved PWV observations. All MODIS NIR PWV pixels were classified into two groups according to the cloud mask of each pixel. For each group, MODIS NIR PWV products and ground-based PWV data from 453 GPS sites in Australia from January 2017 to December 2018 were utilized to determine the differential PWV by subtracting GPS PWV from MODIS PWV. Then, empirical regression relationship between the differential PWV data and the MODIS PWV products was developed using a linear regression approach. The LinearDP model coefficients were independently obtained from each month for each group. The period for model validation spans from January to December in 2019. Comparison of calibrated MODIS NIR PWV versus GPS-derived PWV over Australia showed that the root-mean-square error (RMSE) of Aqua has reduced 42.61% for clear group, 41.43% for cloudy group, and 41.45% for both clear and cloudy groups; and has respectively reduced 53.76%, 37.03%, and 39.33% for Terra. By comparing against ERA5 PWV data, the RMSE reduced 37.21%–43.14% for Aqua and 38.73%–53.87% for Terra. The improvement of MODIS NIR PWV products is further validated in China, with an RMSE reduction of 24.53%–31.78% for Aqua and 28.26%–38.69% for Terra against reference PWV from 214 GPS stations. The mean bias was reduced to −0.415–0.752 mm in Australia and to −0.382–2.013 mm in China.**

***Index Terms*—GPS, lineardp, moderate resolution imaging spectroradiometer (MODIS), near-infrared, precipitable water vapor (PWV).**

I. Introduction

WATER vapor is one of the most important atmospheric components in the climate system [1], [2], [3]. It plays a prominent role in atmospheric circulation [4], [5], energy transportation [6], and meteorological and hydrological processes [7], [8], which in return exerts a fundamental effect on both regional and global climate change [9]. It also indirectly contributes to the formation of clouds when the evaporation from ocean and inland waters is increased due to the rise of the Earth's temperature [10], [11]. It is an essential parameter in numerical weather prediction models and other applications [12], [13], [14], [15], [16]. Based on the ground-based water vapor observations, Sharifi et al. [12] utilized the three-dimensional (3-D) variational (3DVAR) data assimilation system of the weather research and forecasting (WRF) model to perform rainfall prediction. The results showed that the mean absolute error of the accumulated precipitation was reduced about 5% and 13% in 24 h model simulation of February and September cases, respectively. Manandhar et al. [14] proposed a data-driven machine learning method to predict rainfall using several parameters including water vapor, and the validation results indicated that this approach can present a true detection rate of 80.4% as well as a false alarm rate of 20.3%, with an overall accuracy of 79.6%. A common observation of the total water vapor content in the Earth's atmosphere is the precipitable water vapor (PWV), defined as the total atmospheric water vapor contained in a vertical column of the cross-section unit [17], [18]. Since atmospheric water vapor distribution varies greatly in space and time [19], [20], high-quality continuous PWV observations are critical to study the Earth's climate system.

Several ground-based measurement instruments have been utilized to observe PWV, e.g., radiosonde [21], [22], [23] and Global Positioning System (GPS) [24], [25], [26]. Radiosonde and GPS are two widely used and also powerful *in situ* techniques to obtain PWV information. But radiosonde PWV observations usually have a low temporal resolution, typically two observations per day [20], [27], [28]. In contrast, GPS can provide continuous PWV observations at high temporal resolution throughout the day-time and night-time in all weather conditions [20], [29]. The GPS PWV observations also have a higher spatial resolution compared with radiosondes, because the density of *in situ* GPS sites is usually higher than that of radiosondes [29]. In addition, the ground-based GPS PWV measurements showed a good agreement with the *in situ* radiosonde PWV

Manuscript received 8 December 2021; revised 17 March 2022, 18 May 2022, and 29 July 2022; accepted 27 August 2022. Date of publication 7 September 2022; date of current version 21 September 2022. This work was supported in part by the Hong Kong Research Grants Council under Project B-Q80Q PolyU 15221620, and in part by the Emerging Frontier Area Scheme of Research Institute for Sustainable Urban Development of The Hong Kong Polytechnic University under Grant 1-BBWJ. *(Corresponding author: Zhizhao Liu.)*

The authors are with the Department of Land Surveying and Geo-Informatics, The Hong Kong Polytechnic University, Hung Hom 999077, Hong Kong and with the Research Institute for Sustainable Urban Development, The Hong Kong Polytechnic University, Hung Hom 999077, Hong Kong (e-mail: 20074506r@connect.polyu.hk; lszzliu@polyu.edu.hk).

Digital Object Identifier 10.1109/JSTARS.2022.3204823

measurements, with accuracy better than 2 mm [20]. Consequently, GPS measurements of atmospheric water vapor have been widely employed as a reliable reference to evaluate PWV measurements retrieved from satellite instruments [30], [31], [32], [33], [34], [35].

Satellite remote sensing instruments provide another powerful technique to observe PWV. The satellite-based measurements can observe PWV at a global scale using visible [36], NIR [37], [38], [39], infrared (IR) [40], [41], and microwave bands [42], [43]. Nevertheless, the visible or NIR band information is usually sensitive to the clouds in the sun-surface-sensor path, which can result in large uncertainty in the retrieval of space-based PWV observations when there is a presence of clouds [36], [38].

In addition, the reanalysis PWV datasets provided by the European Centre for Medium-Range Weather Forecasts (ECMWF) [44], [45], the Japanese 55-year Reanalysis (JRA-55) [46], [47], and National Center for Environmental Prediction/National Center for Atmospheric Research (NCEP/NCAR) [48], [49], can also be employed to estimate atmospheric water vapor distribution at large spatial scales. The reanalysis PWV data have been reported to be used as the reference to evaluate against other PWV observation techniques [50], [51].

Among various satellite-retrieved remote sensing PWV products, the Moderate Resolution Imaging Spectroradiometer (MODIS), developed by the National Aeronautics and Space Administration (NASA), provides PWV products using NIR bands information at a spatial resolution of 1000 m [52]. The MODIS instrument on-board the Aqua satellite was launched on May 4, 2002, and the one on-board the Terra satellite was launched on December 18, 1999 [53]. The MODIS NIR PWV products from the Aqua and Terra satellites (i.e., MYD05 for Aqua and MOD05 for Terra) are retrieved using 2-channel and 3-channel ratio approaches [52]. Three NIR water vapor absorption channels located at 905, 936, and 940 nm and two NIR window channels at 865 and 1240 nm are utilized. The MYD05 and MOD05 are available over land, ocean, and clouds areas with sun glint [52].

MODIS NIR PWV products have a larger error when data are collected over dark surfaces or under cloudy conditions [52]. Comparison of the MODIS/Terra NIR PWV products against *in situ* GPS-derived PWV data in North America showed an overall root-mean-square error (RMSE) of 5.480 mm under clear conditions, but showed an overall RMSE of 13.066 mm under cloudy conditions [54]. This is mainly because the NIR channels of MODIS instrument are sensitive to the clouds. To the best of our knowledge, there has been no publication related to the improvement of the accuracy of the MODIS NIR PWV products under cloudy conditions.

Some calibration approaches have been developed to improve the accuracy of the PWV product from MODIS NIR bands. In the work by Bai et al. [55], a climate type-related calibration method was proposed to improve the accuracy of the official MODIS NIR PWV products, and the results showed that the RMSE of the original MODIS NIR PWV product was overall reduced by around 20%. Zhu et al. [56] developed a grid-based calibration model to enhance the performance of the MODIS NIR PWV measurements, which implies that the model can reduce RMSE by 53% to 0.6–4.3 mm. However, these calibration models are utilized to improve the accuracy of the MODIS NIR PWV products under confident clear conditions [55], [56]. In addition, several calibration algorithms were developed to enhance the accuracy of satellite-based IR PWV products using differential PWV data, under all-weather conditions. For instance, Chang et al. [57] proposed a cloud mask-related differential linear adjustment model (CDLAM) to improve the all-weather accuracy of the IR PWV products from the MODIS sensor. The results indicated that the CDLAM model can greatly enhance the all-weather accuracy of the MODIS IR PWV products with RMSE reduction in the range between 22% and 51%. They also developed a differential linear adjustment model (DLAM) to enhance the accuracy of IR PWV product from the Atmospheric Infrared Sounder (AIRS) instrument, with RMSE reduced by around 16% [58]. Both CDLAM and DLAM methods employed the ECMWF reanalysis PWV data to calibrate the satellite-based IR PWV products [57], [58]. The performance of these calibration methods for satellite-based NIR and IR PWV products was generally validated with the training data, not using an independent dataset that was observed at a different time [55], [56], [57], [58].

In this study, we proposed a linear differential PWV (LinearDP) calibration model to improve the accuracy of the official MODIS NIR PWV products under both clear and nonclear conditions using ground-based high accuracy GPS-derived PWV data. The *in situ* GPS PWV data were utilized to calculate the differential water vapor information by subtracting reference GPS-derived PWV data from the official MYD05 or MOD05 PWV products. All MODIS NIR PWV pixels were categorized into two groups (clear group and cloudy group) based on the cloud-mask of each pixel. For each group, the regression relationship between the differential PWV and the official MODIS NIR PWV products was determined with a linear regression method, and the empirical model parameters were estimated for each month. In contrast to previous differential PWV-based calibration approaches (CDLAM and DLAM), our LinearDP model utilized GPS PWV as the reference PWV to calibrate the MODIS NIR PWV products under all-weather conditions. Our model was developed for the MODIS NIR PWV products, which is different from both CDLAM and DLAM employed for the satellite-based IR PWV products. We calibrated the MODIS NIR PWV products more frequently (monthly), which is supposed to have better calibration performance. The LinearDP model performance was independently evaluated against an independent dataset, which was independently observed in at a different time and region. Our LinearDP approach for MODIS NIR PWV products is developed based on our regression results after trying different functions (linear, quadratic, and exponential), which is different from the CDLAM or DLAM model relying on a linear relationship assumption between differential PWV and satellite IR PWV products [57], [58].

Section II provides a detailed description of the study region and the datasets used in this research. The methodologies for ground-based GPS water vapor retrieval and the LinearDP approach to improve the MODIS NIR PWV products are presented in Section III. The evaluation metrics used for model validation

TABLE I
SUMMARY OF DATA CHARACTERISTICS USED FOR MODEL DEVELOPMENT AND EVALUATION COLLECTED DURING THE PERIOD BETWEEN JANUARY 1, 2017 AND DECEMBER 31, 2019 OVER AUSTRALIA AND CHINA

Data source	Time Span	Temporal resolution	Spatial resolution	Function	Region
GPS data	January 1, 2017–December 31, 2018	hourly	453 sites, point data	model development	Australia
MODIS geolocation product		daily or	1000 m		
MODIS cloud mask product		twice	1000 m		
MODIS NIR PWV product		daily	1000 m		
GPS data	January 1, 2019–December 31, 2019	hourly	667 sites, point data	model validation	Australia, and China
MODIS geolocation product		daily or	1000 m		Australia, and China
MODIS cloud mask product		twice	1000 m		Australia, and China
MODIS NIR PWV product		daily	1000 m		Australia, and China
ECMWF PWV product		hourly	31 km		Australia

are also shown. In Section IV, the validation results between the calibrated MODIS NIR PWV data against GPS-retrieved reference PWV observations and ECMWF reanalysis PWV data are described. The discussion of the evaluation results is presented in Section V. Section VI gives the conclusions of this article.

II. STUDY AREA AND DATA

A. Study Region

This study region covers two areas: Australia and China, with latitude from 10°41' S to 43°39' S and longitude from 112°57' E to 153°45' E in Australia, and with latitude from 16°42' N to 53°33' N and longitude from 73°40' E to 135°03' E in China. As the study region covers both tropical and mid-latitude areas, the characteristics of climates and land surface covers vary widely from place to place. In particular, the climate in Australia is usually humid and temperate, which is a representative climate in the Southern Hemisphere region [59]. The China includes arid, cold, polar, and temperate climate [60], a representative in the Northern Hemisphere region.

In this region, a total of 667 ground-based stations, equipped with both GPS receivers and meteorological observation device, were selected. In Australia, 453 of the ground-based GPS sites were employed for the development and validation of PWV calibration model. The other 214 GPS stations were located in China and they were utilized to further evaluate the accuracy of the calibrated MODIS NIR PWV data. The calibrated MODIS PWV were retrieved after employing the calibration model developed using the Australian GPS PWV data. The spatial distribution of the 667 ground-based GPS sites is displayed in Fig. 1.

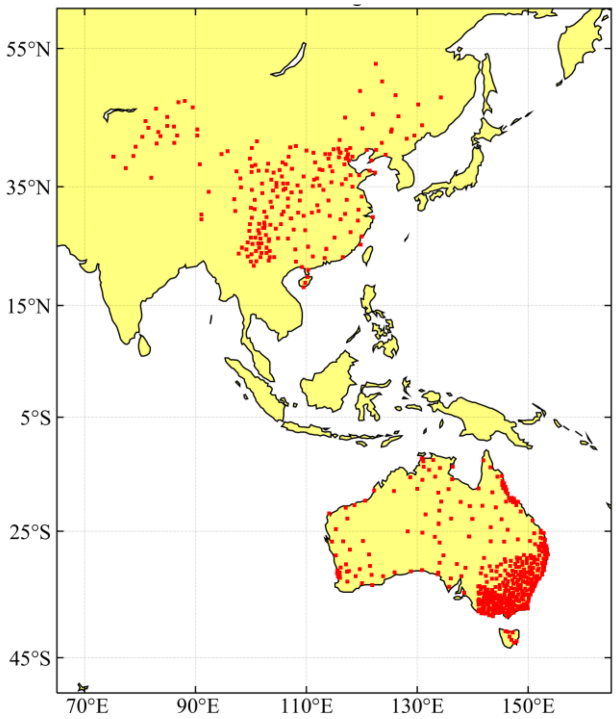

Fig. 1. Geographic location of the *in situ* GPS sites over Australia and China. 453 of these sites are located in Australia, and 214 stations are situated in China.

B. Data

Three types of datasets were employed to develop and evaluate the calibration model in this study, i.e., GPS-derived PWV data, MODIS-derived PWV data, and reanalysis PWV product. The detailed characteristics of the datasets used in this study are presented in Table I.

1) GPS-Derived PWV Data: In this article, the PWV data were hourly estimated from ground-based GPS measurements and they were regarded as the reference to develop and evaluate the new calibration model. The PWV retrieval is based on the zenith total delay (ZTD) products, which were provided by Geoscience Australia for the GPS stations in Australia [61] and Crustal Movement Observation Network of China (CMONOC) for the GPS stations in China [62]. The detailed description of this PWV retrieval approach is given in Section III. As shown in Table I, the two-year GPS-retrieved PWV data from January 1, 2017 to December 31, 2018 from 453 stations in Australia were utilized to establish the new LinearDP calibration model. The GPS-derived PWV data between January 1, 2019 to December 31, 2019 from 453 sites in Australia and 214 sites in China were used as reference PWV to evaluate the performance of the new LinearDP calibration model.

Considering the PWV highly variable feature in time, we require the time difference between two collocated data sources, i.e., GPS and MODIS observations, be smaller than 30 min.

2) MODIS Data: The MODIS is a radiometer sensor on board the Aqua and Terra satellites, launched on 4 May, 2002 and 18 December, 1999, respectively [53]. It observes the Earth in 36 spectral bands ranging in wavelength from 0.4 to 14.4 μm and at varying spatial resolutions from 250 to 1000 m [18]. The MODIS instrument can collect imagery of the same area on Earth approximately 3 h apart, and the entire Earth's surface can be imaged every one to two days [18], [53].

Five NIR channels, including three NIR water vapor absorption channels at 905, 936, and 940 nm and two NIR window channels centered at 865 and 1240 nm, are employed to retrieve atmospheric water vapor over areas with sun glint, e.g., land areas, oceanic areas, and clouds [52]. The water vapor retrieval approach relies upon the 2-channel and 3-channel ratios of radiance from three NIR absorption channels and two NIR window channels [52]. As presented in Table I, three pairs of MODIS data products from both Aqua and Terra satellites were used in this work. They are geolocation product (MYD03/MOD03) [63], PWV product (MYD05/MOD05) [64], and cloud mask product (MYD35/MOD35) [65]. These products have identical spatial resolution of 1000 m. For each MODIS NIR PWV pixel, the geolocation field from MYD03/MOD03 was utilized to obtain the precise geographic location information, and the cloud-mask flag from MYD35/MOD35 was used as a quality control to obtain the clear confidence level information. The MODIS cloud mask product has four conditions according to clear level, namely, Confident Clear (probability >99%), Probably Clear (>95%), Probably Cloudy (>66%), and Confident Cloudy (≤66%) [65].

Two-year MODIS data observed from January 1, 2017 to December 31, 2018 over Australia were employed to construct the new LinearDP calibration model. One-year MODIS data from January 1, 2019 to December 31, 2019 over both Australia and China were utilized for the validation of the LinearDP calibration model.

3) Reanalysis PWV Data: The reanalysis PWV data from ECMWF during the period from January 1, 2019 to December 31, 2019 over Australia (see Table I) were utilized as another reference to evaluate the performance of the proposed LinearDP calibration model. The fifth generation of ECMWF Reanalysis (ERA5) [66], [67] PWV data were selected as they have higher spatiotemporal resolution (31 km × 31 km; hourly) [55] than their predecessor ERA-Interim (79 km × 79 km; 6 hourly) [44]. In addition, ERA5 reanalysis PWV data showed a higher accuracy than JRA-55 and NCEP/NCAR PWV data, after comparing with GPS reference PWV data [69].

III. Methodology

A. Retrieval of Ground-Based Water Vapor Data Using GPS Measurements

The signals between GPS satellites and GPS receivers are usually delayed by the troposphere. This signal propagation delay in the neutral atmosphere is called slant tropospheric delay (STD), which can be converted to zenith total delay (ZTD) using a mapping function [70]. ZTD can be estimated in GPS data analysis. Theoretically, ZTD can be further decomposed into zenith hydrostatic delay (ZHD) and zenith wet delay (ZWD). The ZHD can be estimated as follows [70]:

$$ZHD = (2.2997 \pm 0.0024)\ P_0 / f(\varphi, H) \tag{1}$$

where P_0 is the pressure (hPa) at the height of the ground-based GPS station and $f(\varphi, H)$ is a function for the correction due to gravity changes and can be expressed as [70]

$$f(\varphi, H) = 1 - 0.00266 \cos 2\varphi - 0.00028H \tag{2}$$

where φ and H are the latitude and height (km) of *in situ* GPS site, respectively. The ZWD can be obtained by subtracting the ZHD from the ZTD, from which GPS PWV data can be derived using the equation as follows [70]:

$$PWV = \Pi \cdot ZWD \tag{3}$$

where Π is a scale parameter, which can be estimated from the water vapor weighted mean temperature [71]. It is written as [70]

$$\Pi = \frac{10^6}{\rho R \left(\frac{k_3}{T_m} + k'_2 \right)} \tag{4}$$

where

$$k'_2 = k_2 - mk_1 \tag{5}$$

and ρ is the density of liquid water vapor, 10^3 kg/m^3; R is the gas constant of water vapor, 461 J/kg/K; k_3 is the refraction constant, 3.776×10^5 K^2/hPa; k'_2 is the refraction constant, 16.48 K/hPa; k_1 and k_2 are physical constants; m is the ratio of the water vapor gas constant and the dry air gas constant; and T_m is the water vapor weighted mean temperature.

The water vapor weighted mean temperature (T_m) can be computed from the surface temperature (T_s) at the GPS station using a simple linear model [70]

$$T_m = aT_s + b \tag{6}$$

where coefficients a and b are 0.72 and 70.2, respectively [70], [72].

Normally, T_m can be obtained in two methods: (a) taking surface temperature from meteorological stations and use Bevis formula shown in (6); (b) using partial pressure of water vapor and temperature from reanalysis data such as ERA5 and computing T_m by numerical integration at all pressure/geopotential levels from the surface to the top of the atmosphere. T_m calculated from both (a) and (b) methods can be used to calculate Π in (4). Results show that both (a) and (b) can produce comparable PWV. The RMSE between GPS PWV calculated method (a) and GPS PWV calculated using method (b) is in the range of 0.1–0.7 mm in the tropics and in the range of 0.1–0.3 mm in the polar region [71].

The use of method (a) is much simpler and more computationally saving than method (b). However, it requires *in situ* observation of surface temperature and many GNSS stations do not have meteorological sensors to make *in situ* temperature measurement. In this work, our method is to obtain the surface temperature data for method (a) from ERA5 rather than *in situ* observation. We analyzed the PWV data obtained using our

method (a) and using method (b) from GNSS data in Australia in January 2017 (see supplementary material). It shows that the GPS PWV difference between the two sets of PWV is very small. The RMSE difference is around 0.285 mm. This clearly shows that our method of calculating T_m using (6) and getting meteorological data from ERA5 has an accuracy comparable with method (b).

In this article, the reanalysis meteorological data, i.e., atmospheric pressure and surface temperature from ERA5 reanalysis, were used to estimate the ZHD and the coefficient Π. Considering that the heights between ERA5 and GPS measurements are usually different, the ERA5 data, namely atmospheric pressure and temperature, were corrected to the GPS station level in order to accurately estimate PWV retrievals from GPS observations, which is based on a cubic convolution interpolation approach [73]. In the GPS PWV retrieval process, we require that the spatial distance between ERA5 data and GPS data not exceed 50 km and that the temporal difference between them not exceed 30 min. No interpolation of ERA5 data has been performed. The ZTD products from 667 GPS stations of Geoscience Australia [61] and CMONOC in China [62] were used to retrieve ground-based PWV data for model development and evaluation.

B. Development of the LinearDP Model for Improving MODIS NIR PWV Products

In order to improve the retrieval accuracy of the operational MODIS NIR PWV products, a LinearDP calibration model was developed using ground-based GPS water vapor data in this research. The model to calibrate MODIS NIR PWV products is based on the regression fitting between the differential PWV data and the official MODIS NIR PWV products, where the differential PWV data are estimated by subtracting the GPS-derived PWV data from the official MODIS NIR PWV products. The main steps for the development of the calibration model are summarized as follows.

1) Classification of MODIS NIR PWV Pixels: The MODIS cloud mask product has classified the MODIS pixels into four groups according to probability of clear conditions, i.e., Confident Clear (probability >99%), Probably Clear (>95%), Probably Cloudy (>66%), and Confident Cloudy (≤66%) [65]. In this research, the MODIS NIR PWV pixels were grouped into two categories using the MODIS cloud-mask flags: cloudy group and clear group. PWV pixels with cloud-mask flags of "Confident Cloudy" or "Probably Cloudy" were classified as the "cloudy" group; by contrary, PWV pixels with cloud-mask flags of "Confident Clear" or "Probably Clear" were classified as the "clear" group. For each group, the MODIS NIR PWV pixels closest to *in situ* GPS stations were employed to develop the calibration model in this study, and their spatial distance is required to be smaller than 10 km. Temporally, we require the time difference between two collocated data sources, i.e., GPS and MODIS observations, be smaller than 30 min. This may reduce the error caused by the PWV spatial variation between MODIS and GPS observations [32], [74].

2) Calculation of Differential Water Vapor Data: The *in situ* GPS-retrieved PWV data were first matched with the official MODIS NIR PWV products according to the spatial and temporal criteria. Differential water vapor data were then calculated from these two sets of PWV data by subtracting the reference GPS-derived PWV observations from the MODIS PWV products. It is defined as

$$\Delta PWV = PWV_{MODIS} - PWV_{GPS} \tag{7}$$

where ΔPWV is the calculated differential PWV data; PWV_{MODIS} is the official MODIS NIR PWV product; and PWV_{GPS} is the reference GPS-derived PWV observation.

3) Regression Analysis: An empirical regression relationship between the differential PWV data and the official MODIS NIR PWV products independently was developed for both cloudy and clear groups. The empirical regression was developed separately for both MODIS/Aqua and MODIS/Terra satellites. The PWV data observed over Australia from January 1, 2017 to December 31, 2018 were utilized as training datasets in the regression analysis. The regression results are displayed in Fig. 2. For both MODIS/Aqua and MODIS/Terra satellites, a linear equation can be mathematically developed to characterize the empirical regression relationship between the differential PWV data and the official MODIS NIR PWV products, namely LinearDP calibration model. It is defined as

$$\Delta PWV = a \cdot PWV_{MODIS} + b \tag{8}$$

where a and b are the regression coefficients.

It should be mentioned that, in the presence of clouds, the MODIS NIR water vapor varied in a large range with a poor retrieval accuracy. Thus the ΔPWV had a large variation, as shown in the Fig. 2(b) and (d). Apparently this was because of the effect of clouds on MODIS NIR PWV retrieval process. As a result, the retrieved MODIS NIR water vapor data over clouds varied greatly with poor accuracies.

4) Calculation of LinearDP Model Parameters: Considering the seasonal periodicity of the atmospheric water vapor [32], [54], in this study the coefficients of the LinearDP model were calculated on a monthly basis using the training datasets, i.e., the official MODIS NIR PWV products and the GPS-retrieved PWV data from January 1, 2017 to December 31, 2018 over Australia. It will reduce the seasonal effect on the LinearDP regression model coefficients. The monthly model coefficients were calculated for MODIS/Aqua and MODIS/Terra NIR PWV products as well as two groups of data. Fig. 3 displays an example of the monthly regression model parameters for the MODIS/Terra NIR PWV products for the clear group.

5) Calculation of the Calibrated MODIS NIR PWV Products: After estimating monthly regression coefficients, i.e., a and b in (8), we can determine the monthly calibrated differential water vapor value, ΔPWV_c, using (8) and the official MODIS NIR PWV products. Once the differential PWV data ΔPWV_c are obtained, we can calibrate the official MODIS NIR PWV products by subtracting the differential PWV data:

$$PWV_c = PWV_{MODIS} - \Delta PWV_c \tag{9}$$

where PWV_c is the calibrated MODIS NIR PWV data.

In this LinearDP model, the key step is to estimate the regression parameters a and b using the official MODIS NIR

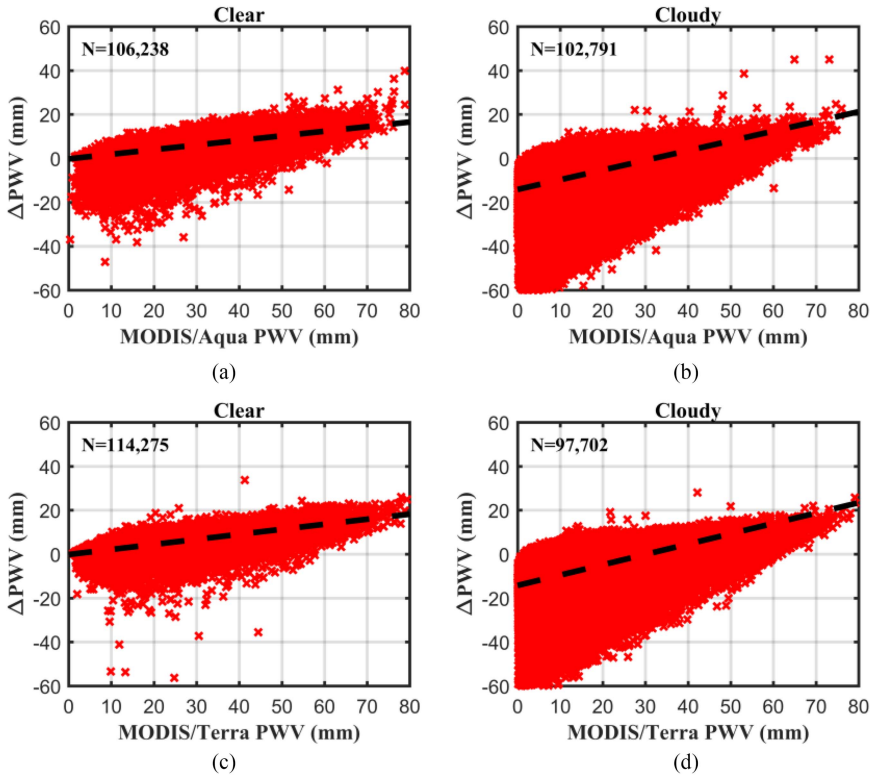

Fig. 2. Regression analysis between the differential PWV data against the official MODIS NIR PWV products. The spatiotemporally collocated MODIS-GPS PWV data sources during the period from January 1, 2017 to December 31, 2018 over Australia were selected for regression analysis. (a) and (b) Scatter points of the differential PWV data versus the official MODIS/Aqua NIR PWV products for clear and cloudy groups. (c) and (d) Scatter points of the differential PWV data versus the official MODIS/Terra NIR PWV products for clear and cloudy groups. *N* represents the number of collocated data points used for regression analysis. The dashed black lines represent the empirical regression fitting.

PWV products and the reference ground-based GPS-retrieved PWV data. These two sets of PWV data from January 1, 2017 to December 31, 2018 over Australia were employed to estimate the monthly model coefficients.

C. Evaluation Metrics

The calibrated MODIS NIR PWV data, namely PWV_c, were evaluated on a pixel-by-pixel basis against two types of reference PWV data, i.e., *in situ* GPS-derived PWV data and reanalysis ERA5 PWV data. Only MODIS NIR PWV pixels closest to each ground-based GPS station were selected for model evaluation. Three statistical metrics were employed to evaluate the performance of the calibration model: coefficient of determination (R^2), RMSE, and mean bias (MB). Equations for these performance assessment metrics are given as follows:

$$R^2 = \left[\frac{\sum_{i=1}^{n} \left(PWV_o - \overline{PWV}_o\right)\left(PWV_r - \overline{PWV}_r\right)}{\sqrt{\sum_{i=1}^{n} \left(PWV_o - \overline{PWV}_o\right)^2 \left(PWV_r - \overline{IWV}_r\right)^2}} \right]^2 \tag{10}$$

$$RMSE = \sqrt{\frac{1}{n} \sum\nolimits_{i=1}^{n} \left(PWV_o - PWV_r\right)^2} \tag{11}$$

$$MB = \frac{1}{n} \sum_{i=1}^{n} \left(PWV_o - PWV_r\right) \tag{12}$$

where PWV_o represents the observed PWV which are official MODIS PWV products or calibrated MODIS PWV; $\overline{PWV}_o$ represents the mean observed PWV; PWV_r represents the reference PWV data from GPS or ERA5 model; $\overline{PWV}_r$ represents the mean reference PWV data, and n represents the number of data pairs. R^2 and RMSE show the difference between the MODIS PWV data against the reference PWV data. MB indicates if MODIS-observed PWV data have been overestimated or underestimated against the reference PWV data.

IV. Results

To study if the LinearDP model could improve the accuracy of the official MODIS NIR PWV products, the calibrated MODIS PWV data were evaluated by comparing against reference ground-based GPS-derived PWV data and reanalysis ERA5 PWV data in Australia. The calibrated MODIS PWV data were also assessed in China by comparing with reference *in situ* GPS-retrieved PWV data. The calibrated MODIS PWV data in this article were calculated using the monthly coefficients of the empirical regression functions, which were monthly estimated

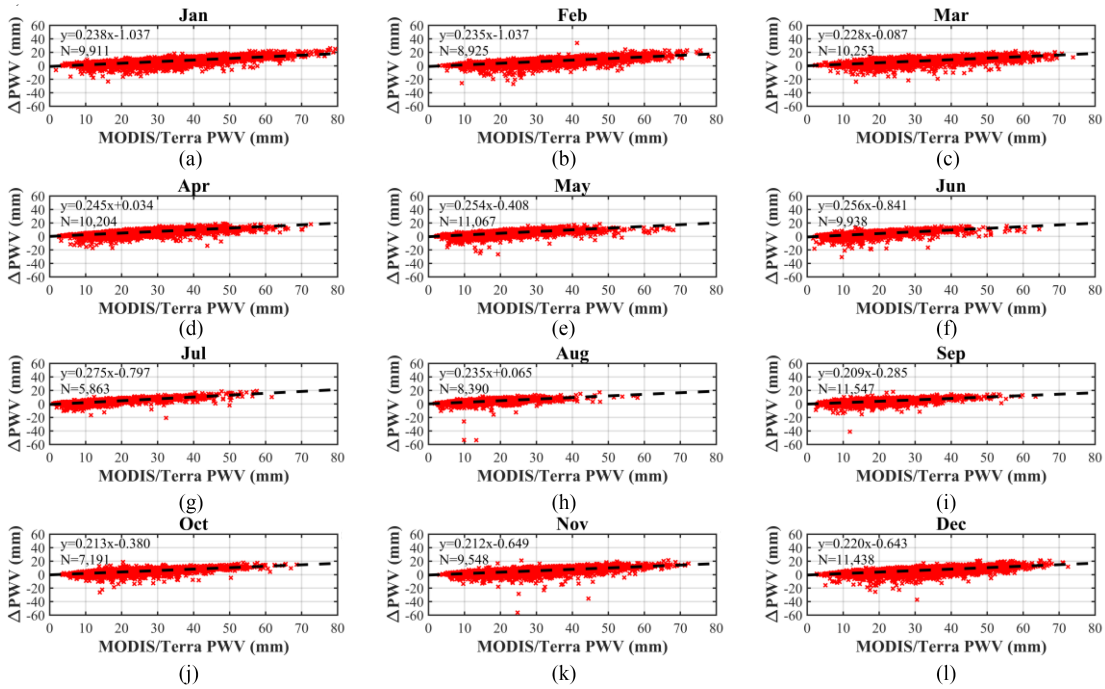

Fig. 3. Example of the calculated monthly model parameters between the differential PWV data against the official MODIS/Terra NIR PWV products in clear group. The spatiotemporally collocated MODIS-GPS PWV data sources during the period from January 1, 2017 to December 31, 2018 over Australia were selected for the calculation of the monthly regression model coefficients. *N* represents the number of spatiotemporally collocated data points used for calculating monthly regression model parameters. The dashed black lines represent the linear regression of these data.

using the training datasets: the official MODIS NIR PWV products and *in situ* GPS-retrieved PWV data collected over Australia from January 1, 2017 to December 31, 2018.

A. Evaluation of the Calibrated MODIS NIR PWV Products Using GPS-Derived Reference PWV Data in Australia

The calculated monthly model coefficients were employed to calibrate the official MODIS NIR PWV products observed over Australia from January 1, 2019 to December 31, 2019. The calibrated MODIS NIR PWV data were then evaluated using *in situ* reference PWV data from 453 GPS sites over Australia. The evaluation results were displayed in Figs. 4 and 5, showing that the calibrated MODIS NIR PWV data had superior accuracy than the operational MODIS NIR PWV products.

The results showed that for the clear group, the RMSE was reduced by 42.61% from 4.813 to 2.762 mm for Aqua satellite, and by 53.76% from 5.506 to 2.546 mm for Terra satellite. For the cloudy group, the RMSE was reduced by 41.43% from 14.574 mm to 8.536 mm, and 37.03% from 14.376 mm to 9.053 mm. For all MODIS NIR PWV pixels obtained from both clear and cloudy groups, the RMSE was reduced by 41.45% from 10.533 to 6.167 mm, and by 39.33% from 10.413 to 6.318 mm.

After using the LinearDP model developed in this research, the MB was also reduced. The MB values were much close to 0 for both Aqua and Terra satellites. Meanwhile, the strength of the correlation relationship between the calibrated MODIS NIR PWV data and the reference GPS-observed PWV data was also improved, with the slopes and offsets closer to 1 and 0, respectively.

The evaluation results were further discussed in a monthly basis. As shown in Table II, the official MODIS NIR PWV products were also improved in each month in terms of the RMSE reduction. The monthly maximum RMSE reduction was in January for Aqua satellite and in March for Terra satellite. The RMSE was reduced by 45.94% from 14.865 to 8.036 mm in January for Aqua satellite and by 49.25% from 16.245 to 8.336 mm in March for Terra satellite. The monthly minimum RMSE reduction occurred in August for both Aqua and Terra satellites, with an RMSE reduction of 29.68% from 5.478 to 3.852 mm for Aqua satellite and 29.89% from 6.149 to 4.311 mm for Terra satellite. The monthly slopes and offsets of the linear regression lines between the calibrated MODIS NIR PWV data and ground-based GPS-derived PWV data were much closer to 1 and 0, respectively, compared with the official MODIS NIR PWV products. For both Aqua and Terra satellites, the monthly MB values tended to approach 0 when the calibration model was applied. For both clear and cloudy group, the quality of monthly metrics (R^2, RMSE, and MB) was also enhanced after the application of the calibration model, with higher correlation, smaller RMSE, and lower MB against reference GPS PWV data [see Fig. 6(a)–(f)]. Fig. 6(g) and (h) show that in each month, the number of MODIS NIR PWV data that were enhanced after the LinearDP calibration was significantly higher than that was worsened after the LinearDP calibration, for both clear and cloudy groups.

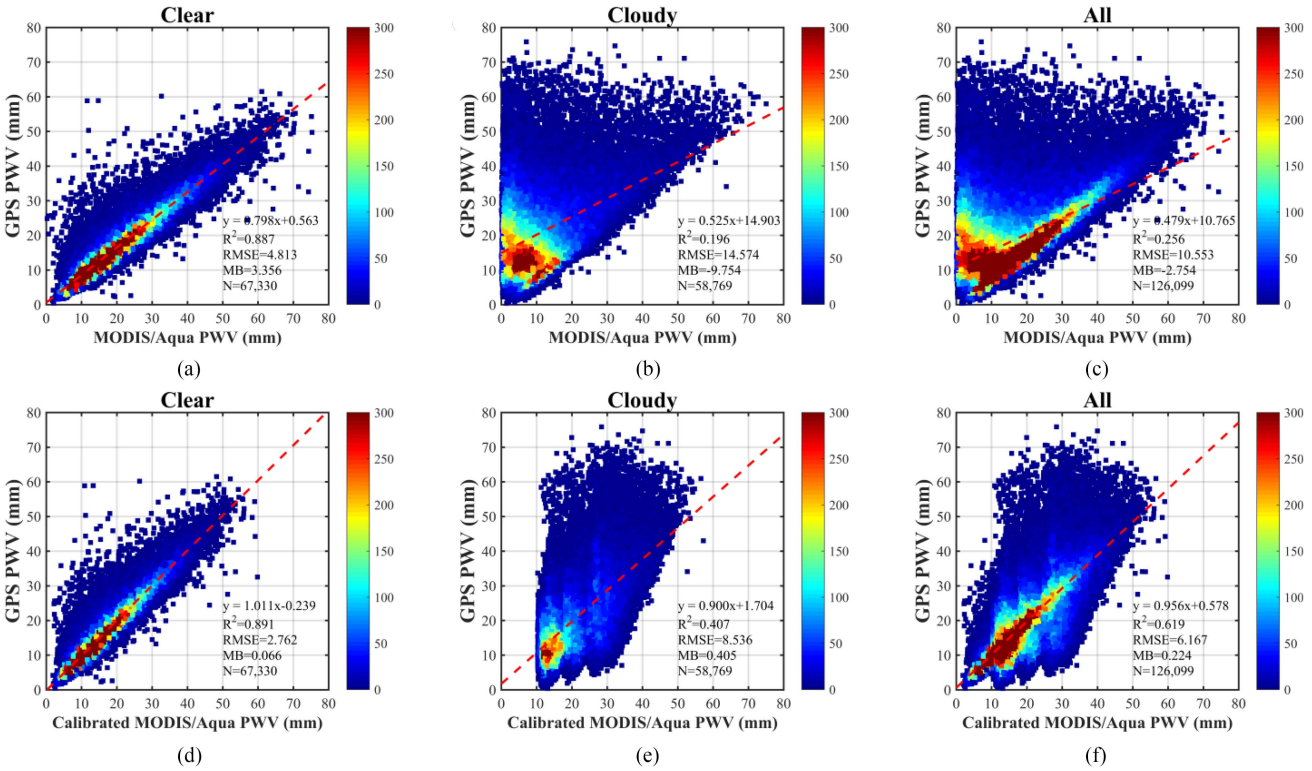

Fig. 4. Evaluation of the PWV data calculated from MODIS/Aqua measurements versus the *in situ* GPS-retrieved PWV data from January 1, 2019 to December 31, 2019 over Australia. (a)–(c) Scatter plots between the official MODIS/Aqua NIR PWV products and the ground-based GPS-derived PWV data for clear group, cloudy group, and all MODIS NIR PWV pixels, respectively. (d)–(f) Scatter plots between the calibrated MODIS/Aqua NIR PWV products and the ground-based GPS-derived PWV data for clear group, cloudy group, and all MODIS NIR PWV pixels, respectively. All MODIS NIR pixels are obtained from both clear and cloudy groups. *N* represents the number of spatiotemporally collocated MODIS-GPS data points selected for the comparison analysis. The dashed red lines represent the linear regression results of these data. The points colored with a rainbow scale illustrate the frequency of the MODIS NIR PWV values (brown most frequent, blue least frequent).

In addition, we showed in Figs. 7 and 8 the station-based R^2, RMSE, MB values between MODIS NIR PWV and GPS PWV from January 1, 2019 to December 31, 2019 over Australia. The PWV values measured from the clear group were utilized. The accuracies of both MODIS/Aqua and MODIS/Terra NIR PWV products were improved with the employment of the LinearDP model. In particular, the station-based RMSE was generally reduced to below 4 mm in most GPS stations, lower than the original MODIS NIR PWV products that usually had an RMSE of more than 4 mm. The station-based MB for the original MODIS NIR PWV products was often above 2 mm in most GPS stations. With the use of the LinearDP model, the station-based MB values at most GPS stations were usually reduced to −1–2 mm. In most GPS stations, the R^2 values of the original MODIS NIR PWV products were comparable to those of the calibrated MODIS NIR PWV products.

B. Evaluation of the Calibrated MODIS NIR PWV Products Using Reference Reanalysis PWV Data in Australia

To further evaluate the performance of the LinearDP model developed model in this study, the accuracy of the calibrated MODIS NIR PWV data collected over Australia between January 1, 2019 and December 31, 2019 were also compared against ECMWF ERA5 PWV data. The locations used for PWV comparison were based on the geographic locations of the *in situ* 453 GPS stations in Australia.

The results displayed in Figs. 9 and 10 suggested that the calibration model developed in this work significantly improved the retrieval accuracy of the MODIS NIR PWV products. For Aqua satellite, the LinearDP model reduced the RMSE by 37.21% from 4.708 to 2.956 mm for clear group, by 43.14% from 14.918 to 8.482 mm for cloudy group, and by 42.51% from 10.749 to 6.180 mm for all MODIS/Aqua NIR PWV pixels. For the Terra satellite, the model reduced RMSE by 53.87% from 5.389 to 2.486 mm for clear group, by 38.73% from 14.636 to 8.967 mm for cloudy group, and by 40.70% from 10.539 to 6.250 mm all MODIS/Terra NIR PWV pixels. The slopes for Aqua satellite improved from 0.773 to 0.980 after calibration for clear group, from 0.510 to 0.890 for cloudy group, and from 0.462 to 0.937 for all MODIS/Aqua NIR PWV pixels. The corresponding offsets changed from 1.521 to 0.736 for clear group, from 15.539 to 2.371 for cloudy group, and from 11.502 to 1.505 for all MODIS/Aqua NIR PWV pixels. Similarly, the slopes and offsets of the linear regression lines for Terra satellite were much closer to 1 and 0.

The monthly comparison between the MODIS NIR PWV data and the reference ERA5 PWV data was performed, with results displayed in Table III. For Aqua satellite, the monthly maximum RMSE reduction was 49.39% from 16.85 to 8.528

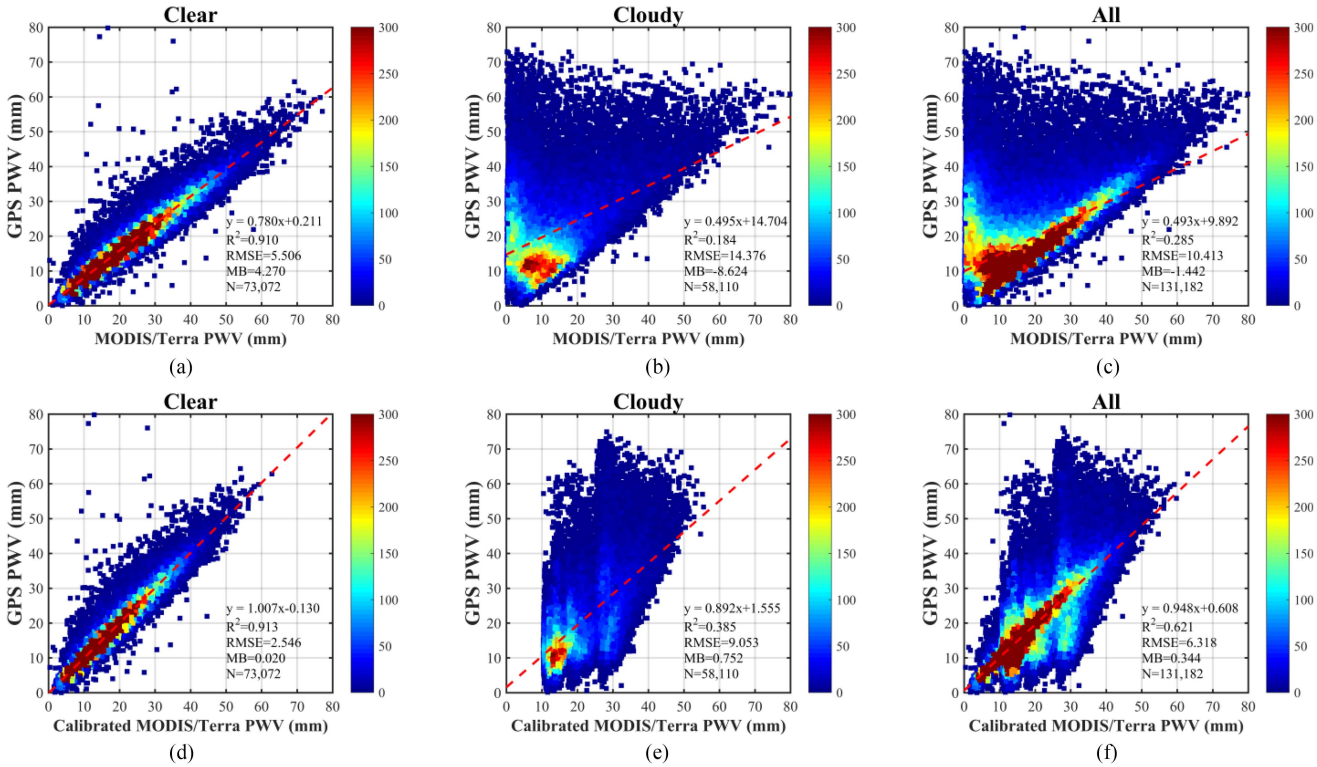

Fig. 5. Evaluation of the PWV data calculated from MODIS/Terra measurements versus the *in situ* GPS-retrieved PWV data from January 1, 2019 to December 31, 2019 over Australia. (a)–(c) Scatter plots between the official MODIS/Terra NIR PWV products and the ground-based GPS-derived PWV data for clear group, cloudy group, and all MODIS NIR PWV pixels, respectively. (d)–(f) Scatter plots between the calibrated MODIS/Terra NIR PWV products and the ground-based GPS-derived PWV data for clear group, cloudy group, and all MODIS NIR PWV pixels, respectively. All MODIS NIR pixels are obtained from both clear and cloudy groups. *N* represents the number of spatiotemporally collocated MODIS-GPS data points selected for the comparison analysis. The dashed red lines represent the linear regression results of these data. The points colored with a rainbow scale illustrate the frequency of the MODIS NIR PWV values (brown most frequent, blue least frequent).

mm in March, and the minimum RMSE reduction was 32.35% from 10.243 to 6.929 mm in May. For Terra satellite, the monthly maximum RMSE reduction was 47.29% from 15.063 to 7.940 mm in January, and the monthly minimum RMSE reduction was 30.63% from 5.432 to 3.768 mm in August. After LinearDP calibration, the monthly slopes and offsets for both Aqua and Terra satellites were much closer to 1 and 0, respectively. The monthly MB values were closer to 0 too after calibration. With the employment of the calibration method, the monthly R^2, RMSE, and MB were improved for both clear and cloudy groups compared to the original MODIS NIR PWV products, as displayed in Fig. 11. For both clear and cloudy groups, many more data points showed an improvement after the LinearDP calibration than those showing an accuracy degradation.

Figs. 12 and 13 show the station-based comparison results between the PWV data from MODIS clear group and ERA5 from January 1, 2019 to December 31, 2019 over Australia. It can be seen that the LinearDP calibration method can enhance the performance of the PWV observations at MODIS NIR bands at most GPS stations. The station-based RMSE for the original MODIS NIR PWV products was often above 3 mm at most stations, while for the calibrated MODIS NIR PWV data the station-based RMSE at most stations was usually below 3 mm. The station-based MB was generally reduced to −1–1 mm at most stations, better than the original MODIS NIR PWV products with MB values of more than 1 mm at most stations. For R^2, the original MODIS NIR PWV products showed a very similar magnitude with the calibrated MODIS NIR PWV products, at most GPS stations.

C. Evaluation of the Calibrated MODIS NIR PWV Products Using Reference GPS PWV Data in China

In addition to Australia, the LinearDP calibration model was also evaluated in a different regions, i.e., China. This allows a more comprehensive evaluation of the performance of the calibration model in different geographical regions. In this article, the calibrated MODIS NIR PWV data over China were derived from the monthly regression model coefficients for the period January 1, 2019 to December 31, 2019. A total of 214 GPS stations over China were used in this comparison analysis. As shown in Section III, the monthly regression model coefficients were estimated from the training datasets over Australia during January 1, 2017 to December 31, 2018.

Considering the seasonal difference between China and Australia, the monthly regression model parameters used for China region need to match the ones of Australia with similar meteorological characteristics. The LinearDP model coefficients in

TABLE II
MONTHLY EVALUATION AGAINST REFERENCE GPS-RETRIEVED PWV DATA DURING THE PERIOD FROM JANUARY 1, 2019 TO DECEMBER 31, 2019 OVER AUSTRALIA.

	PWV product	Aqua					Terra				
		Slope	Offset	R^2	RMSE	MB	Slope	Offset	R^2	RMSE	MB
Jan	MYD05/MOD05	0.302	20.112	0.134	14.865	-1.921	0.311	20.005	0.136	14.248	-3.111
	Calibrated MYD05/MOD05	0.964	0.838	0.530	8.036	0.177	0.948	1.004	0.557	7.507	0.452
Feb	MYD05/MOD05	0.369	16.459	0.163	13.003	-1.631	0.366	17.027	0.171	13.234	-3.093
	Calibrated MYD05/MOD05	0.942	0.844	0.537	7.701	0.648	0.973	0.449	0.585	7.165	0.240
Mar	MYD05/MOD05	0.239	21.162	0.082	16.113	-5.033	0.235	21.809	0.076	16.425	-6.922
	Calibrated MYD05/MOD05	0.968	0.569	0.420	8.815	0.278	0.994	0.195	0.457	8.336	-0.031
Apr	MYD05/MOD05	0.372	12.595	0.198	10.674	-1.061	0.305	15.160	0.110	12.102	-4.034
	Calibrated MYD05/MOD05	1.054	-0.794	0.452	6.738	-0.243	1.093	-1.061	0.400	7.372	-0.729
May	MYD05/MOD05	0.334	11.389	0.126	10.202	-1.634	0.352	11.536	0.127	10.079	-2.965
	Calibrated MYD05/MOD05	1.070	-0.052	0.366	6.930	-1.022	1.083	-0.604	0.335	6.932	-0.678
Jun	MYD05/MOD05	0.286	10.631	0.106	8.919	-1.822	0.313	10.966	0.117	9.048	-3.118
	Calibrated MYD05/MOD05	0.978	0.548	0.351	5.654	-0.240	0.988	0.559	0.327	5.812	-0.385
Jul	MYD05/MOD05	0.344	8.319	0.170	6.667	-0.421	0.305	9.518	0.121	6.945	-1.799
	Calibrated MYD05/MOD05	0.889	1.154	0.388	4.354	0.264	0.924	1.177	0.386	4.299	-0.207
Aug	MYD05/MOD05	0.515	5.175	0.335	5.478	0.274	0.458	6.498	0.225	6.149	-0.743
	Calibrated MYD05/MOD05	1.017	-0.425	0.526	3.852	0.240	1.091	-1.115	0.460	4.311	0.077
Sep	MYD05/MOD05	0.392	8.025	0.197	6.898	-0.666	0.329	9.375	0.142	7.429	-1.586
	Calibrated MYD05/MOD05	1.008	0.067	0.510	4.257	-0.165	0.998	0.236	0.483	4.341	-0.208
Oct	MYD05/MOD05	0.369	10.120	0.185	7.904	-1.043	0.331	11.127	0.161	8.071	-1.959
	Calibrated MYD05/MOD05	0.834	1.510	0.486	5.074	1.263	0.809	1.865	0.492	4.880	1.384
Nov	MYD05/MOD05	0.452	10.496	0.252	9.538	-2.341	0.402	11.205	0.194	9.479	-2.783
	Calibrated MYD05/MOD05	0.853	1.146	0.548	6.196	1.620	0.884	0.479	0.551	5.768	1.672
Dec	MYD05/MOD05	0.467	11.034	0.316	9.248	-0.368	0.448	11.948	0.269	9.482	-1.456
	Calibrated MYD05/MOD05	0.830	2.058	0.560	6.248	1.706	0.858	1.636	0.569	6.042	1.468

spring months (September, October, and November) in Australia were employed to calculate the calibrated MODIS NIR PWV data in spring months (March, April, and May) in China. Considering the different climates in the two hemispheres, similarly for the other months, a shift of six months needs to be considered.

The evaluation results were presented in Figs. 14 and 15. As shown in Fig. 14, the original and the calibrated MODIS/Aqua NIR PWV products were evaluated using reference *in situ* GPS-derived PWV data. It is clearly found that the overall difference between the MODIS/Aqua NIR PWV products and the reference GPS-retrieved PWV data was reduced after using the LinearDP calibration model, with an RMSE reduction of 31.78% from 4.408 to 3.007 mm for clear group, 24.53% from 14.294 to 10.787 mm for cloudy group, and 24.93% from 11.484 to 8.621 mm for all MODIS NIR PWV pixels from both clear and cloudy groups. The MB values for MODIS/Aqua NIR PWV product were reduced from 2.547 (overestimated) to 0.237 mm (overestimated) for clear group, from −8.323 (underestimated) to 2.013 mm (overestimated) for cloudy group, and from −4.065 (underestimated) to 1.317 mm (overestimated) for all MODIS NIR PWV pixels.

In Fig. 15, the evaluation results of the MODIS/Terra satellites indicated that the LinearDP calibration model developed in this study significantly improved the retrieval accuracy of MODIS/Terra PWV, and reduced the RMSE by 38.69% from 4.451 to 2.729 mm for clear group, by 28.26% from 15.675 to 11.245 mm for cloudy group, and by 28.74% from 12.539 to 8.935 mm for all MODIS/Terra NIR PWV pixels. After calibration, the size of MB value were reduced from 2.648 (overestimated) to −0.382 mm (underestimated) for clear group, from −9.359 (underestimated) to 0.407 mm (overestimated) for

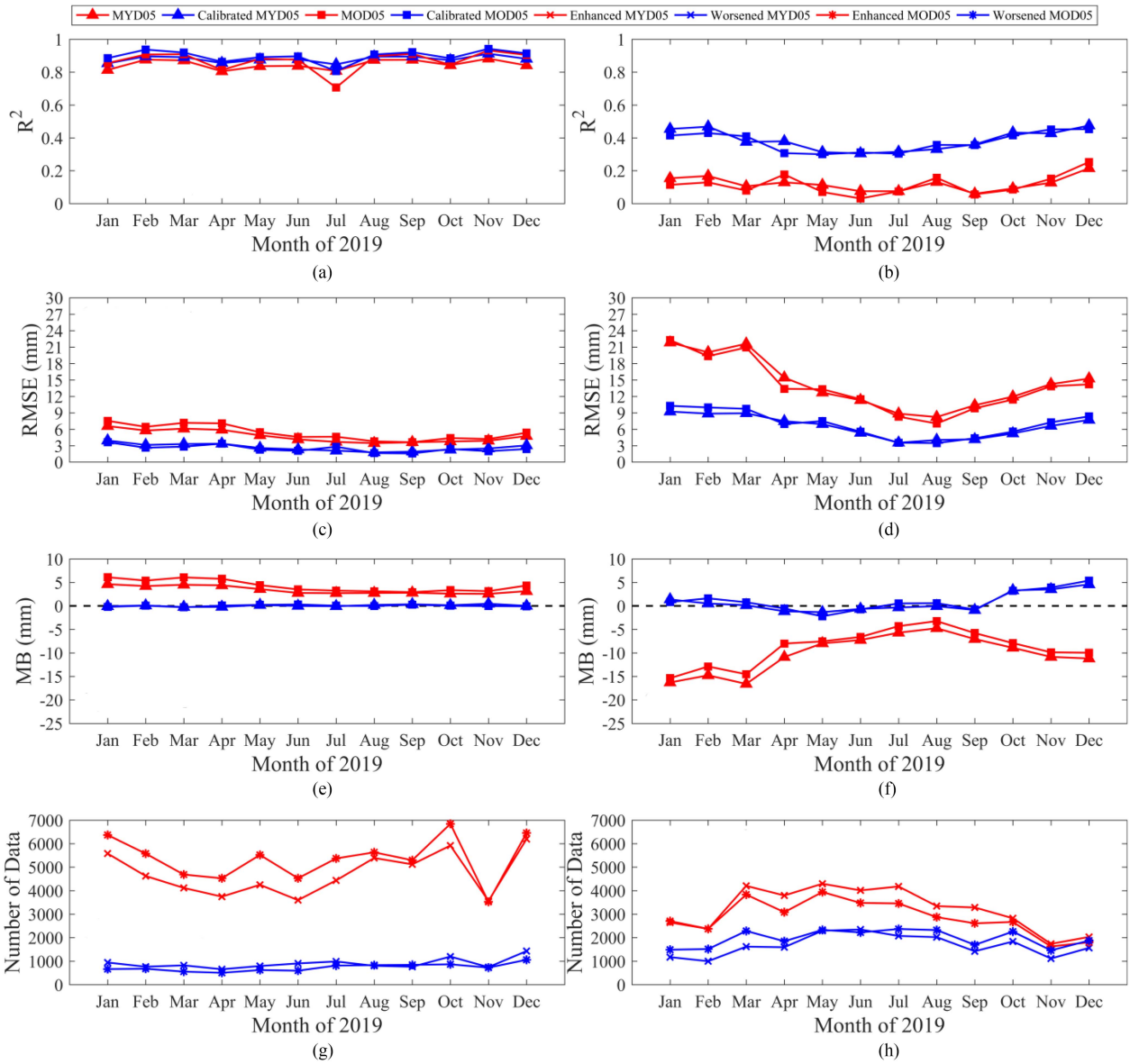

Fig. 6. Monthly comparison of MODIS PWV measurements against reference GPS PWV measurements from January 1, 2019 to December 31, 2019 over Australia, using PWV data from the clear group and cloudy group. (a), (c), (e), and (g) MODIS-measured NIR PWV data versus reference GPS-measured PWV data in clear group. (b), (d), (f), and (h) MODIS-measured NIR PWV data versus reference GPS-measured PWV data in cloudy group.

cloudy group, and from −4.656 (underestimated) to 0.098 mm (overestimated) for all MODIS/Terra NIR PWV pixels.

The significant improvement of the official MODIS/Aqua and MODIS/Terra NIR PWV products in China further confirmed and illustrated the effectiveness of the LinearDP model developed in this study.

In addition, the monthly evaluation analysis was also conducted and shown in Table IV. For MODIS/Aqua NIR PWV products, the monthly maximum RMSE reduction was 44.10% from 19.481 to 10.889 mm in August; the monthly minimum RMSE reduction was 7.92% from 5.262 to 4.845 mm in December. For MODIS/Terra NIR PWV products, the monthly maximum RMSE reduction was 45.39% from 21.926 to 11.974 mm in July, with the monthly minimum RMSE reduction of 5.90% from 5.695 to 5.359 mm in January. After LinearDP calibration, most of the monthly slopes of the linear regression lines for both Aqua and Terra satellites were closer to 1. The monthly MB values were also closer to 0 after calibration. As presented in Fig. 16, the calibrated MODIS NIR PWV data generally showed higher R^2, lower RMSE, and smaller MB with respect to reference GPS PWV data in each month in both clear and cloudy groups. For both clear and cloudy groups, the monthly number of the data improved by the LinearDP calibration method was significantly larger than that worsened by the calibration method.

Moreover, we conducted the station-based comparison between MODIS-based PWV and GPS-based PWV from January 1, 2019 to December 31, 2019 over China, using three evaluation metrics i.e., R^2, RMSE, and MB. The three statistical metrics were estimated utilizing the data from the clear group. The

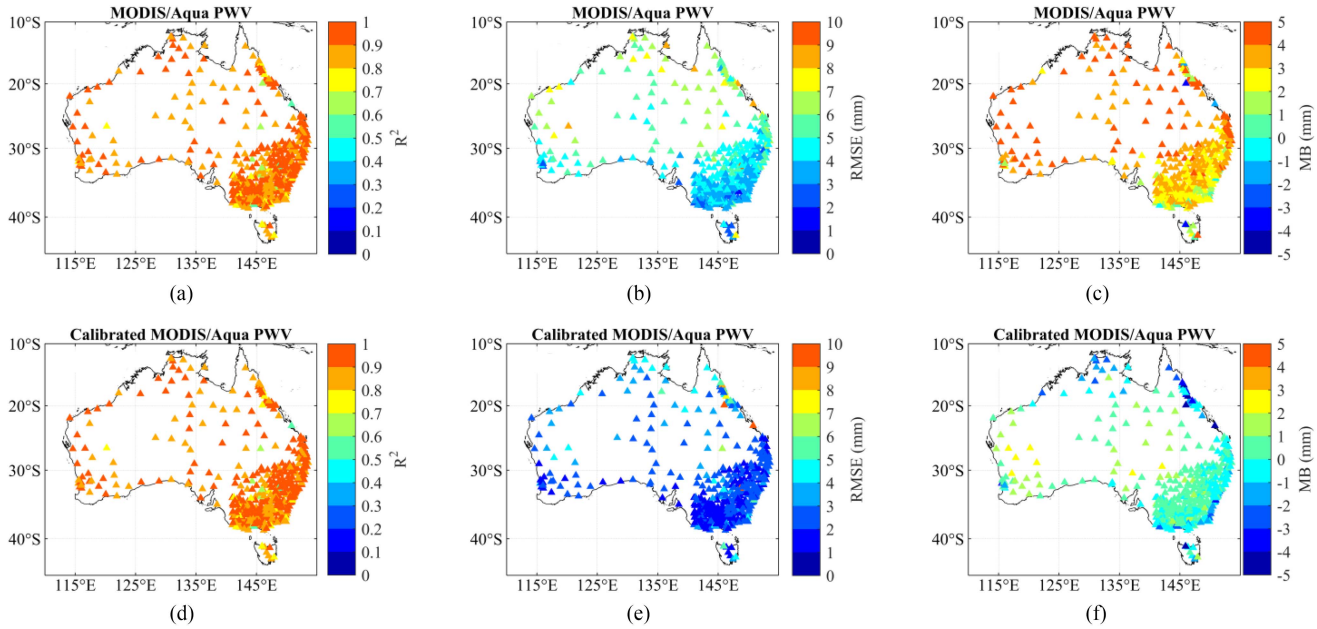

Fig. 7. Annual R^2, RMSE, and MB values for MODIS/Aqua PWV measurements against reference GPS PWV measurements at each GPS station from January 1, 2019 to December 31, 2019 over Australia, using PWV data from the clear group. (a)–(c) Original MODIS/Aqua NIR PWV products versus reference GPS-measured PWV data. (d)–(f) Calibrated MODIS/Aqua NIR PWV products versus reference GPS-measured PWV data.

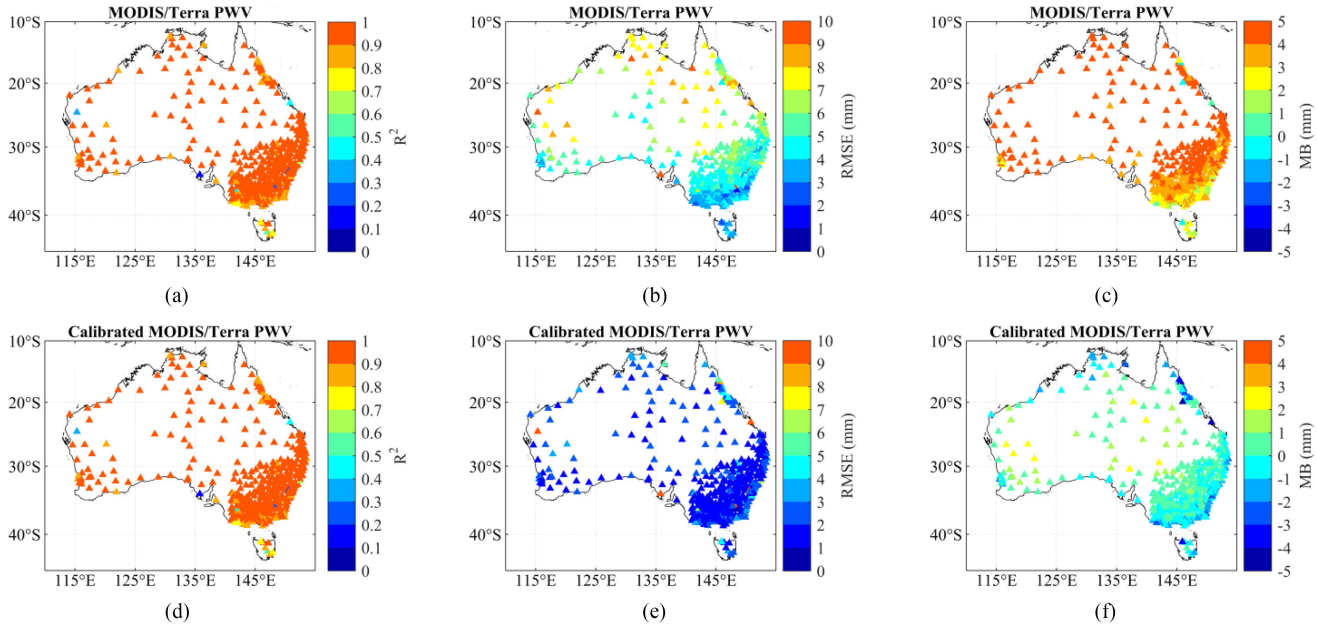

Fig. 8. Annual R^2, RMSE, and MB values for MODIS/Terra PWV measurements against reference GPS PWV measurements at each GPS station from January 1, 2019 to December 31, 2019 over Australia, using PWV data from the clear group. (a)–(c) Original MODIS/Terra NIR PWV products versus reference GPS-measured PWV data. (d)–(f) Calibrated MODIS/Terra NIR PWV products versus reference GPS-measured PWV data.

station-based RMSE and MB at most stations were generally reduced after applying the LinearDP calibration model, as results shown in Figs. 17 and 18. In most GPS stations, the station-based RMSE was usually reduced below 4 mm, with MB reduced in the range between −1 mm and 2 mm. The correlation R^2 of the original MODIS NIR PWV products was comparable to that of the calibrated MODIS NIR PWV products, at most GPS stations.

V. Discussion

High quality water vapor observation through satellite remote sensing instruments is vital in many Earth observation systems. This study proposed a novel empirical LinearDP calibration approach to improve the accuracy of NIR PWV products from MODIS/Aqua (MYD05 products) and MODIS/Terra

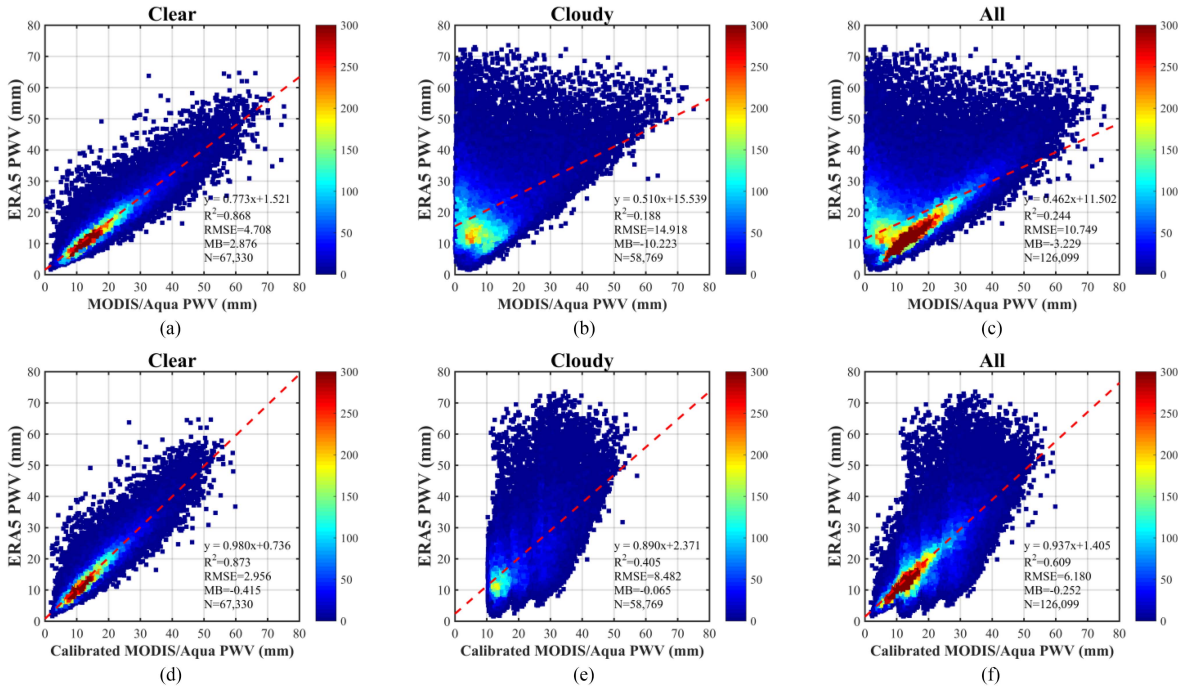

Fig. 9. Evaluation of the PWV data calculated from MODIS/Aqua measurements versus the reanalysis ERA5 PWV data from January 1, 2019 to December 31, 2019 over Australia. (a)–(c) Scatter plots between the official MODIS/Aqua NIR PWV products and the reanalysis ERA5 PWV data for clear group, cloudy group, and all MODIS NIR PWV pixels, respectively. (d)–(f) Scatter plots between the calibrated MODIS/Aqua NIR PWV products and the reanalysis ERA5 PWV data for clear group, cloudy group, and all MODIS NIR PWV pixels, respectively. All MODIS NIR pixels are obtained from both clear and cloudy groups. *N* represents the number of spatiotemporally collocated MODIS-ERA5 data points selected for comparison analysis. The dashed red lines represent the linear regression results of these data. The points colored with a rainbow scale illustrate the frequency of the MODIS NIR PWV values (brown most frequent, blue least frequent).

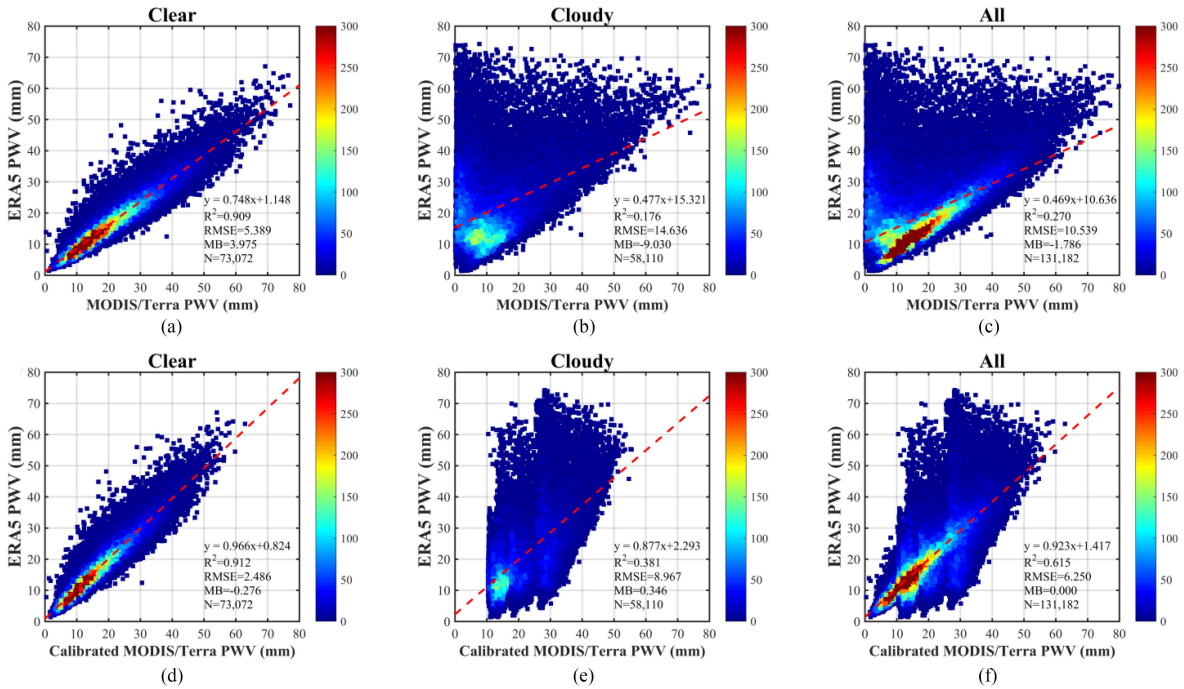

Fig. 10. Evaluation of the PWV data calculated from MODIS/Terra measurements versus the reanalysis ERA5 PWV data from January 1, 2019 to December 31, 2019 over Australia. (a)–(c) Scatter plots between the official MODIS/Terra NIR PWV products and the reanalysis ERA5 PWV data for clear group, cloudy group, and all MODIS NIR PWV pixels, respectively. (d)–(f) Scatter plots between the calibrated MODIS/Terra NIR PWV products and the reanalysis ERA5 PWV data for clear group, cloudy group, and all MODIS NIR PWV pixels, respectively. All MODIS NIR pixels are obtained from both clear and cloudy groups. *N* represents the number of spatiotemporally collocated MODIS-ERA5 data points selected for the comparison analysis. The dashed red lines represent the linear regression results of these data. The points colored with a rainbow scale illustrate the frequency of the MODIS NIR PWV values (brown most frequent, blue least frequent).

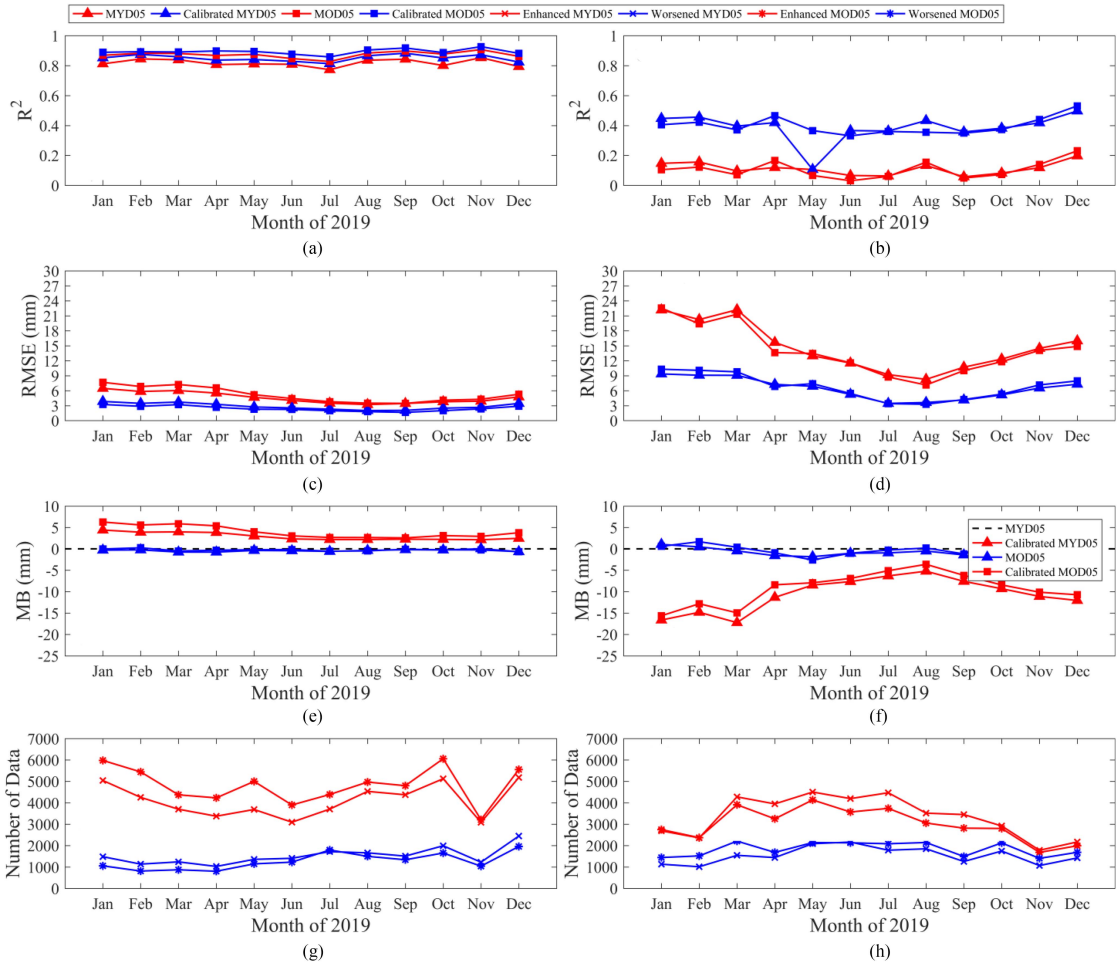

Fig. 11. Monthly comparison of MODIS PWV measurements against reference ERA5 PWV measurements from January 1, 2019 to December 31, 2019 over Australia, using PWV data from the clear group and cloudy group. (a), (c), (e), and (g) MODIS-measured NIR PWV data versus reference ERA5 PWV data in clear group. (b), (d), (f), and (h) MODIS-measured NIR PWV data versus reference ERA5 PWV data in cloudy group.

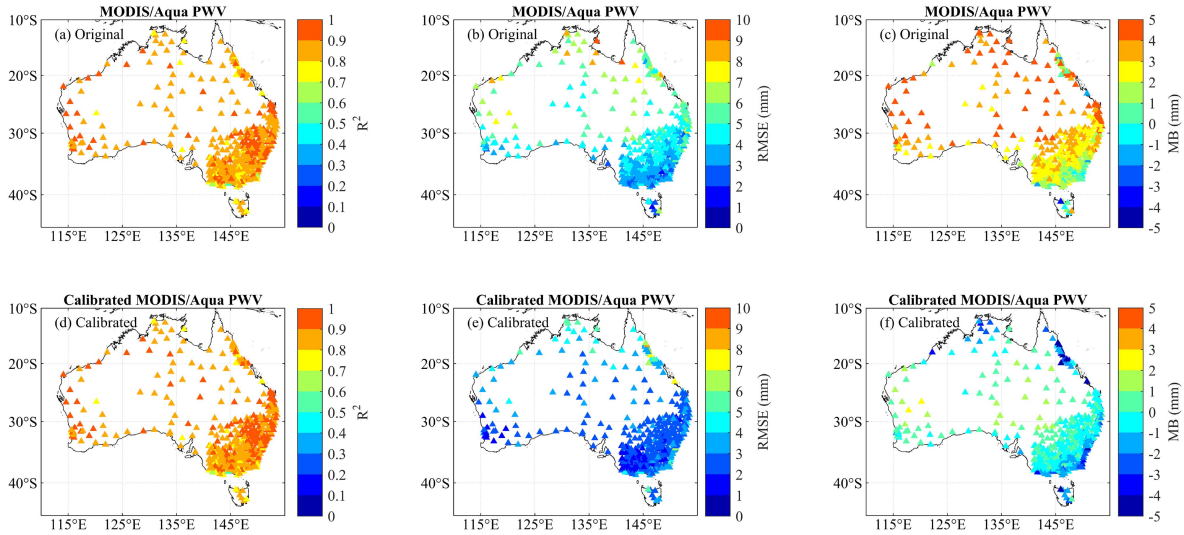

Fig. 12. Annual R^2, RMSE, and MB values for MODIS/Aqua PWV measurements against reference ERA5 PWV measurements at each GPS station from January 1, 2019 to December 31, 2019 over Australia, using PWV data from the clear group. (a)–(c) Original MODIS/Aqua NIR PWV products versus reference ERA5 PWV data. (d)–(f) Calibrated MODIS/Aqua NIR PWV products versus reference ERA5 PWV data.

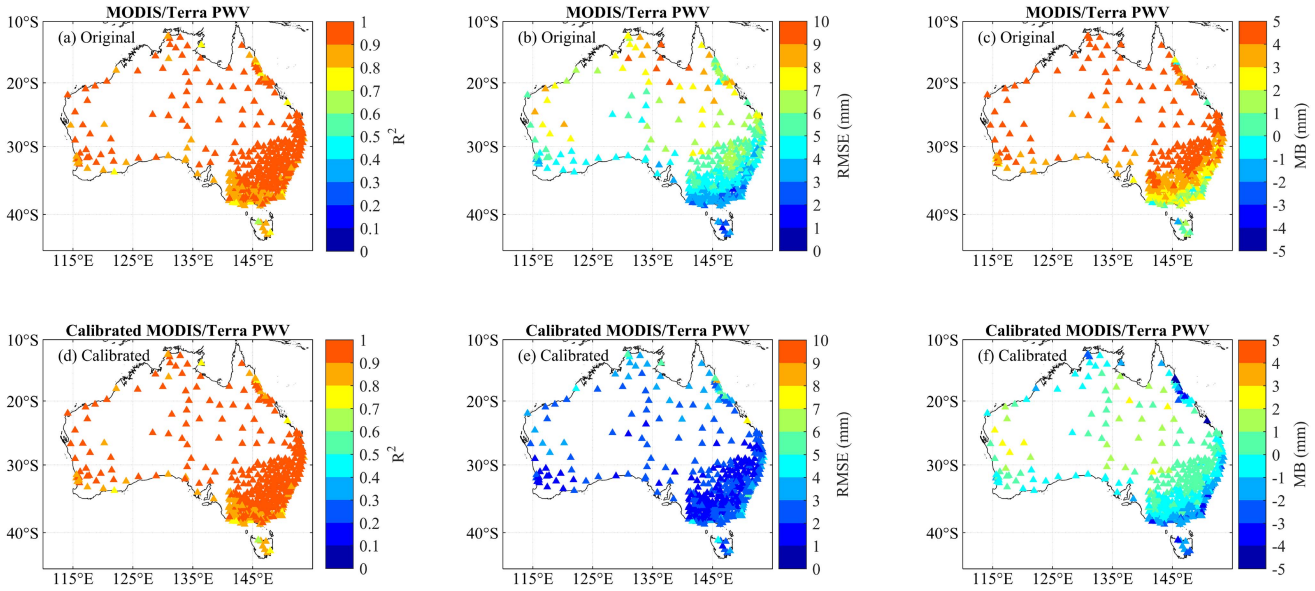

Fig. 13. Annual R^2, RMSE, and MB values for MODIS/Terra PWV measurements against reference ERA5 PWV measurements at each GPS station from January 1, 2019 to December 31, 2019 over Australia, using PWV data from the clear group. (a)–(c) Original MODIS/Terra NIR PWV products versus reference ERA5 PWV data. (d)–(f) Calibrated MODIS/Terra NIR PWV products versus reference ERA5 PWV data.

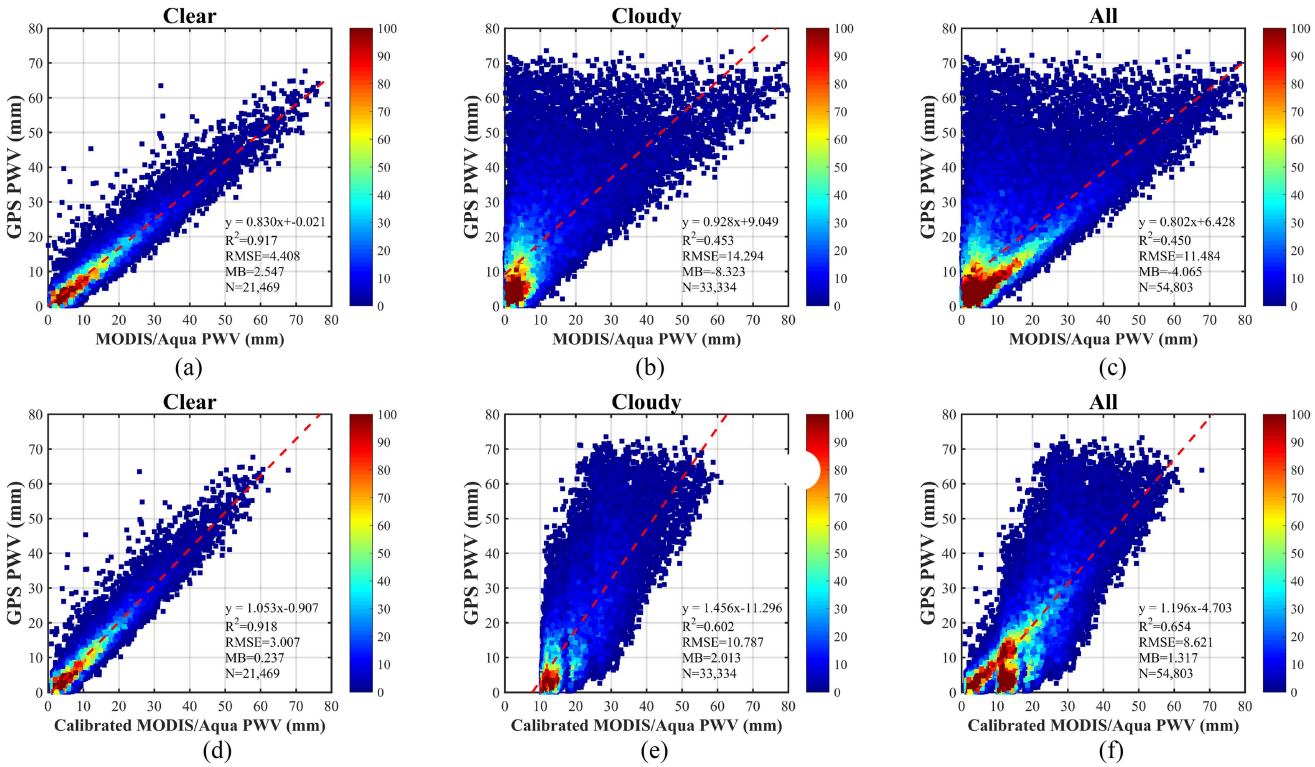

Fig. 14. Evaluation of the PWV data calculated from MODIS/Aqua measurements versus the *in situ* GPS-retrieved PWV data from January 1, 2019 to December 31, 2019 over China. (a)–(c) Scatter plots between the official MODIS/Aqua NIR PWV products and the ground-based GPS-derived PWV data for clear group, cloudy group, and all MODIS NIR PWV pixels, respectively. (d)–(f) Scatter plots between the calibrated MODIS/Aqua NIR PWV products and the ground-based GPS-derived PWV data for clear group, cloudy group, and all MODIS NIR PWV pixels, respectively. All MODIS NIR pixels are obtained from both clear and cloudy groups. *N* represents the number of spatiotemporally collocated MODIS-GPS data points selected for comparison analysis. The dashed red lines represent the linear regression results of these data. The points colored with a rainbow scale illustrate the frequency of the MODIS NIR PWV values (brown most frequent, blue least frequent).

TABLE III
MONTHLY EVALUATION AGAINST REFERENCE ERA5 PWV DATA DURING THE PERIOD FROM JANUARY 1, 2019 TO DECEMBER 31, 2019 OVER AUSTRALIA.

	PWV product	Aqua					Terra				
		Slope	Offset	R^2	RMSE	MB	Slope	Offset	R^2	RMSE	MB
Jan	MYD05/MOD05	0.297	20.627	0.126	14.420	-3.373	0.272	20.877	0.114	15.063	-1.908
	Calibrated MYD05/MOD05	0.931	1.759	0.545	7.546	0.191	0.935	1.650	0.521	7.940	0.189
Feb	MYD05/MOD05	0.356	17.468	0.163	13.375	-3.310	0.348	16.810	0.147	13.158	-1.485
	Calibrated MYD05/MOD05	0.945	1.382	0.555	7.399	0.022	0.920	1.271	0.520	7.810	0.794
Mar	MYD05/MOD05	0.221	22.651	0.067	16.850	-7.504	0.223	21.819	0.072	16.403	-5.346
	Calibrated MYD05/MOD05	0.978	1.197	0.439	8.528	-0.614	0.952	1.295	0.406	8.912	-0.034
Apr	MYD05/MOD05	0.284	15.991	0.102	12.206	-4.526	0.349	13.397	0.190	10.662	-1.447
	Calibrated MYD05/MOD05	1.045	0.356	0.393	7.214	-1.221	1.008	0.467	0.449	6.497	-0.628
May	MYD05/MOD05	0.335	12.300	0.119	10.243	-3.494	0.317	12.038	0.119	10.242	-2.035
	Calibrated MYD05/MOD05	1.042	0.549	0.322	6.929	-1.207	1.034	0.908	0.358	6.876	-1.422
Jun	MYD05/MOD05	0.295	11.573	0.108	9.206	-3.518	0.279	11.108	0.105	8.943	-2.202
	Calibrated MYD05/MOD05	0.951	1.479	0.315	5.793	-0.785	0.943	1.417	0.341	5.609	-0.620
Jul	MYD05/MOD05	0.275	10.437	0.104	7.153	-2.376	0.310	9.411	0.159	6.672	-1.106
	Calibrated MYD05/MOD05	0.881	2.294	0.375	4.283	-0.784	0.852	2.305	0.409	4.026	-0.421
Aug	MYD05/MOD05	0.440	7.210	0.226	6.110	-1.258	0.505	5.709	0.335	5.432	-0.145
	Calibrated MYD05/MOD05	1.053	-0.169	0.468	4.111	-0.438	0.997	0.216	0.526	3.768	-0.180
Sep	MYD05/MOD05	0.307	10.166	0.130	7.584	-2.122	0.368	8.700	0.183	6.963	-1.049
	Calibrated MYD05/MOD05	0.956	1.320	0.465	4.369	-0.745	0.974	0.873	0.504	4.196	-0.548
Oct	MYD05/MOD05	0.305	11.877	0.141	8.297	-2.350	0.331	11.020	0.161	8.034	-1.397
	Calibrated MYD05/MOD05	0.772	2.894	0.460	4.903	0.993	0.806	2.325	0.492	4.824	0.908
Nov	MYD05/MOD05	0.387	11.775	0.184	9.624	-3.141	0.441	10.892	0.240	9.695	-2.571
	Calibrated MYD05/MOD05	0.854	1.386	0.529	5.766	1.315	0.845	1.534	0.539	6.201	1.390
Dec	MYD05/MOD05	0.415	13.297	0.238	9.859	-2.193	0.435	12.301	0.283	9.558	-0.999
	Calibrated MYD05/MOD05	0.833	2.920	0.551	5.983	0.731	0.805	3.241	0.542	6.184	1.075

All MODIS NIR PWV pixels obtained from both clear and cloudy groups were used.

(MOD05 products) under all-weather conditions (both clear and cloudy) based on *in situ* GPS-retrieved PWV data. The relationship between the differential PWV and the official MODIS PWV data was built through an empirical regression. The differential PWV data were calculated by subtracting the GPS-observed water vapor data from the official MODIS PWV products.

The MODIS NIR PWV pixels were grouped into two categories (clear and cloudy) based on the cloud-mask flags of the MODIS cloud mask product [65]. For each category, MODIS PWV products and ground-based GPS PWV data observed over Australia during January 1, 2017 and December 31, 2018 were employed as the training datasets to estimate the empirical regression function.

Considering the variation characteristics of the PWV, the LinearDP regression model coefficients were calculated monthly for each group and each satellite. The accuracy of the model was evaluated by comparing the calibrated MODIS NIR PWV data against reference ground-based GPS-retrieved PWV data as well as ECMWF reanalysis ERA5 PWV products.

MODIS NIR PWV products are affected by clouds, as satellite-based NIR measurements cannot penetrate the clouds [54]. This is different from satellite-based IR PWV products that are little affected by the clouds [32]. The clouds can result in poor quality MODIS NIR PWV data, with an RMSE of larger than 10 mm, as shown in our work and the previous work [54]. The official MODIS NIR PWV products under clear conditions have a higher accuracy than those under cloudy conditions. The accuracy of operational MODIS NIR PWV products generally is in the range of 4 to 6 mm under clear conditions [30], [54], [55]. This level of PWV accuracy still needs to be improved, not to mention the PWV accuracy under cloudy conditions.

By employing our LinearDP approach, the quality of PWV products from MODIS NIR channels was greatly enhanced under both clear and cloudy conditions, obtaining higher correlation, smaller RMSE, and lower MB with respect to reference PWV data.

For calibration results over Australia region, the RMSE reduction for the Aqua satellite was 42.61% from 4.813 to 2.762 mm for the clear group, 41.43% from 14.574 to 8.536 mm for

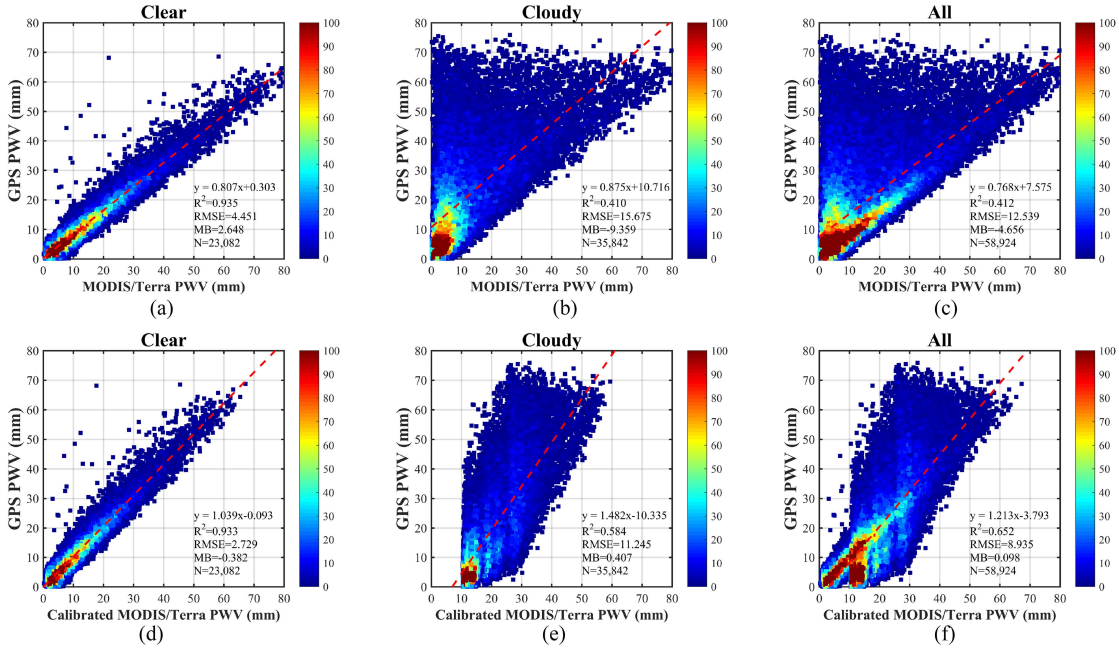

Fig. 15. Evaluation of the PWV data calculated from MODIS/Terra measurements versus the *in situ* GPS-retrieved PWV data from January 1, 2019 to December 31, 2019 over China. (a)–(c) Scatter plots between the official MODIS/Terra NIR PWV products and the ground-based GPS-derived PWV data for clear group, cloudy group, and all MODIS NIR PWV pixels, respectively. (d)–(f) Scatter plots between the calibrated MODIS/Terra NIR PWV products and the ground-based GPS-derived PWV data for clear group, cloudy group, and all MODIS NIR PWV pixels, respectively. All MODIS NIR pixels are obtained from both clear and cloudy groups. *N* represents the number of spatiotemporally collocated MODIS-GPS data points selected for the comparison analysis. The dashed red lines represent the linear regression results of these data. The points colored with a rainbow scale illustrate the frequency of the MODIS NIR PWV values (brown most frequent, blue least frequent).

the cloudy group, and 41.45% from 10.533 to 6.167 mm for all MODIS/Aqua data (both clear and cloudy groups), when compared with reference GPS PWV data. For the Terra satellite, the RMSE was reduced by 53.76% from 5.506 to 2.546 mm for the clear group, 37.03% from 14.376 m to 9.053 mm for the cloudy group, and 39.33% from 10.413 to 6.318 mm for all MODIS/Terra satellite data (both clear and cloudy groups). When compared with ERA5 PWV reference data, the RMSE of the Aqua satellite PWV products has reduced by 37.21% from 4.708 to 2.956 mm for the clear group, 43.14% from 14.918 to 8.482 mm for the cloudy group, and 42.51% from 10.749 to 6.180 mm for all MODIS Aqua data. The RMSE of the Terra satellite PWV products was reduced by 53.87% from 5.389 to 2.486 mm for the clear group, 38.73% from 14.636 to 8.967 mm for the cloudy group, and 40.70% from 10.539 to 6.250 mm for all MODIS Terra data.

For calibration results over China region, the RMSE of MODIS/Aqua PWV products has reduced by 31.78% from 4.408 to 3.007 mm for the clear group, 24.53% from 14.294 to 10.787 mm for the cloudy group, and 24.93% from 11.484 to 8.621 mm for all MODIS/Aqua data, when compared with reference PWV data from 214 GPS stations in China. For the Terra satellite, the RMSE has reduced by 38.69% from 4.451 to 2.729 mm for the clear group, by 28.26% from 15.675 to 11.245 mm for the cloudy group, and by 28.74% from 12.539 to 8.935 mm for all the Terra satellite data.

In terms of RMSE reduction, the performance of the LinearDP model in China was slightly poorer than in Australia, which is probably because the model coefficients were computed from the data collected in Australia. China covers a larger geographical area than Australia. The climatic variation in China is also more significant than Australia. This could also be a factor for the slightly poorer performance of the calibration model in China.

The LinearDP model can greatly improve the all-weather accuracy of the official MODIS NIR PWV products in both Australia and China regions. The good performance of the model in the two representative regions of Southern Hemisphere and Northern Hemisphere indicates that the calibration model can be applied to other similar regions to enhance the accuracy of MODIS NIR PWV measurements under all weather conditions. This LinearDP model can be a promising tool to improve the accuracy of MODIS NIR PWV products and even other satellite-based NIR PWV products.

Our LinearDP calibration model can calibrate MODIS NIR PWV data with an improved accuracy under both clear and cloudy sky conditions, which is different from previously published calibration models that only focused on the calibration of MODIS NIR PWV product under clear sky conditions. Under clear sky conditions, the RMSE reduction in Bai et al. [55] was around 20%. As a comparison, our LinearDP model has reduced RMSE by more than 40% in Australia and more than 30% in China. In recent work by Zhu et al. [56], the accuracy for MODIS NIR PWV products was improved by 53% to 0.6–4.3 mm. However, their model performance was usually validated with the training data, not using an independent dataset that was observed in at a different time. In our research, the model was

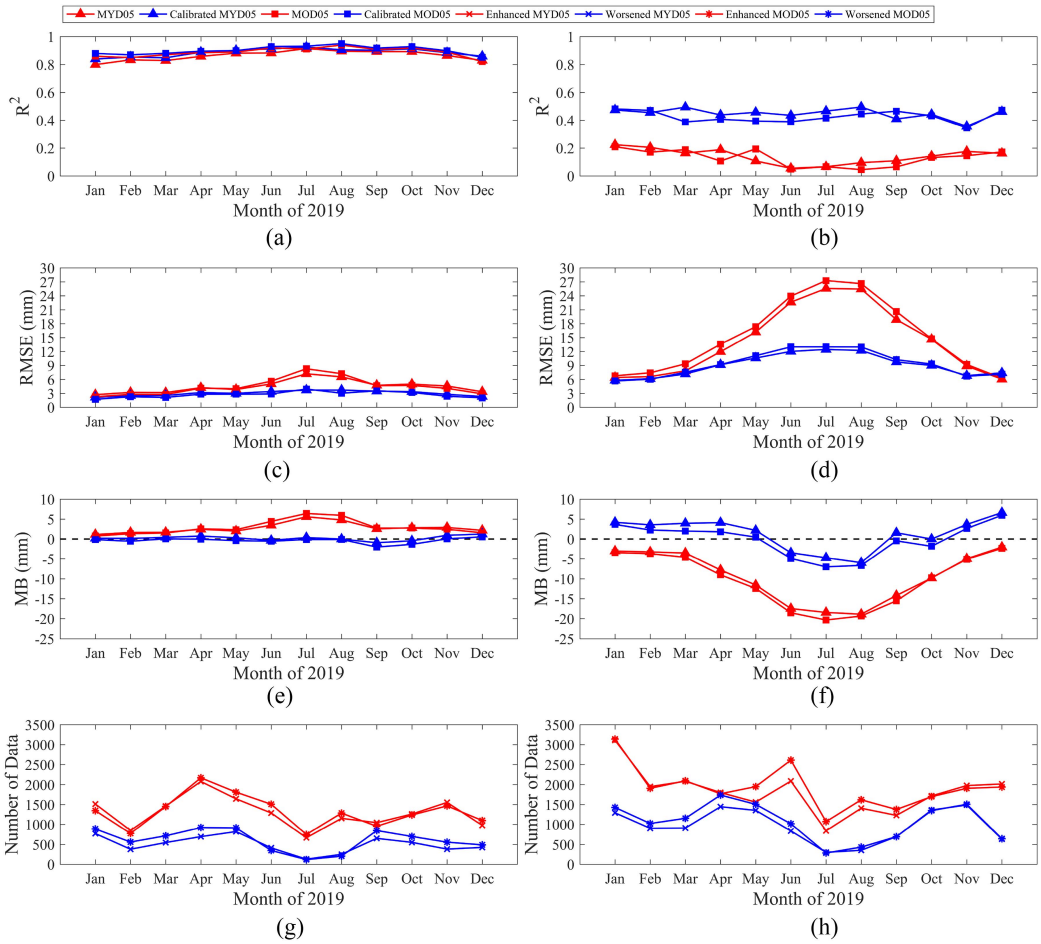

Fig. 16. Monthly comparison of MODIS PWV measurements against reference GPS PWV measurements from January 1, 2019 to December 31, 2019 over China, using PWV data from the clear group and cloudy group. (a), (c), (e), and (g) MODIS-measured NIR PWV data versus reference GPS-measured PWV data in clear group. (b), (d), (f), and (h) MODIS-measured NIR PWV data versus reference GPS-measured PWV data in cloudy group.

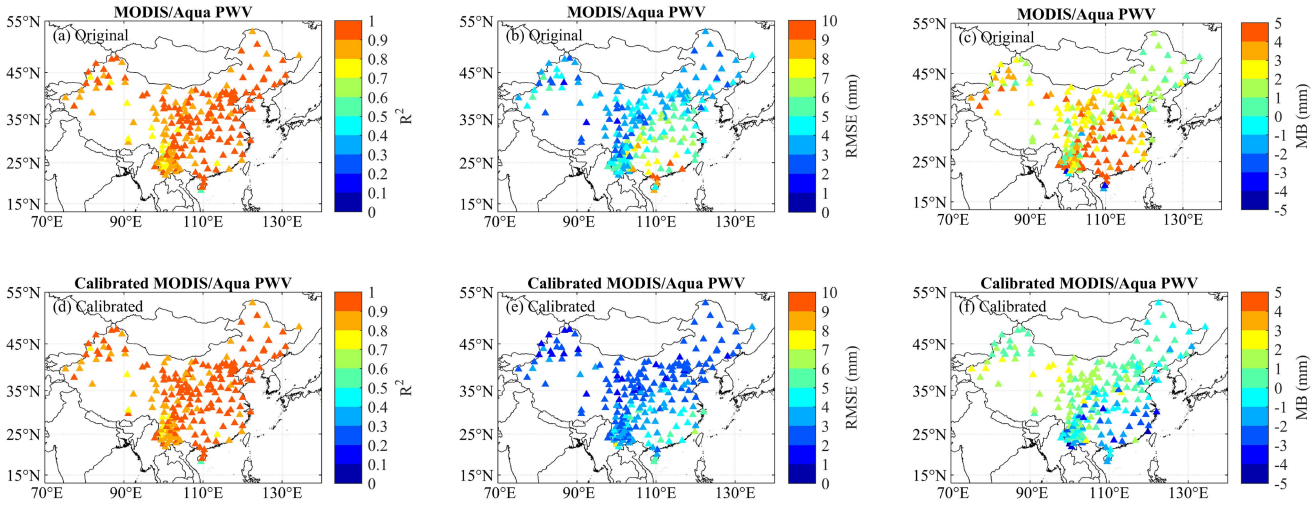

Fig. 17. Annual R^2, RMSE, and MB values for MODIS/Aqua PWV measurements against reference GPS PWV measurements at each GPS station from January 1, 2019 to December 31, 2019 over China, using PWV data from the clear group. (a)–(c) Original MODIS/Aqua NIR PWV products versus reference GPS-measured PWV data. (d)–(f) Calibrated MODIS/Aqua NIR PWV products versus reference GPS-measured PWV data.

TABLE IV
MONTHLY EVALUATION AGAINST REFERENCE GPS-RETRIEVED PWV DATA DURING THE PERIOD FROM JANUARY 1, 2019 TO DECEMBER 31, 2019 OVER CHINA.

	PWV product	Aqua					Terra				
		Slope	Offset	R^2	RMSE	MB	Slope	Offset	R^2	RMSE	MB
Jan	MYD05/MOD05	0.907	2.137	0.506	5.427	-1.605	0.888	2.702	0.505	5.695	-2.061
	Calibrated MYD05/MOD05	0.973	-2.552	0.576	4.445	1.522	0.999	-2.384	0.581	5.359	1.397
Feb	MYD05/MOD05	0.864	2.640	0.496	5.787	-1.777	0.843	3.164	0.471	6.338	-2.118
	Calibrated MYD05/MOD05	1.027	-2.814	0.588	4.945	1.528	1.106	-2.447	0.530	5.777	1.372
Mar	MYD05/MOD05	0.896	2.173	0.466	6.379	-1.434	0.860	3.215	0.403	7.445	-2.152
	Calibrated MYD05/MOD05	1.016	-2.706	0.551	5.264	1.124	1.124	-2.572	0.449	6.503	1.215
Apr	MYD05/MOD05	0.762	5.733	0.441	9.234	-3.082	0.714	7.012	0.376	10.293	-3.603
	Calibrated MYD05/MOD05	1.049	-3.384	0.483	8.468	2.559	1.104	-2.653	0.494	8.378	0.942
May	MYD05/MOD05	0.717	8.961	0.334	12.199	-5.357	0.701	10.029	0.317	13.252	-5.920
	Calibrated MYD05/MOD05	1.147	-4.153	0.480	9.489	1.308	1.165	-3.341	0.487	9.964	0.079
Jun	MYD05/MOD05	0.441	20.448	0.155	18.260	-9.788	0.393	22.526	0.123	19.744	-10.769
	Calibrated MYD05/MOD05	1.324	-6.285	0.461	11.338	-2.32	1.344	-5.763	0.429	12.320	-3.429
Jul	MYD05/MOD05	0.409	24.216	0.201	20.176	-8.586	0.347	26.891	0.154	21.926	-9.917
	Calibrated MYD05/MOD05	1.204	-3.959	0.572	11.336	-2.638	1.177	-1.259	0.560	11.974	-4.328
Aug	MYD05/MOD05	0.351	23.886	0.142	19.481	-8.385	0.308	25.803	0.117	20.786	-8.700
	Calibrated MYD05/MOD05	1.102	0.369	0.537	10.889	-3.317	1.102	0.897	0.515	11.566	-3.896
Sep	MYD05/MOD05	0.534	14.662	0.274	14.142	-6.342	0.478	16.503	0.219	15.410	-7.027
	Calibrated MYD05/MOD05	1.013	-0.724	0.539	8.884	0.395	1.023	0.634	0.533	9.264	-1.188
Oct	MYD05/MOD05	0.633	10.045	0.344	11.997	-5.135	0.648	9.913	0.358	11.888	-4.895
	Calibrated MYD05/MOD05	1.191	-3.333	0.485	8.965	-0.173	1.191	-1.712	0.508	9.055	-1.638
Nov	MYD05/MOD05	0.665	5.098	0.383	7.618	-2.154	0.678	5.235	0.383	7.706	-2.291
	Calibrated MYD05/MOD05	1.006	-2.767	0.392	7.255	1.681	1.000	-1.677	0.394	7.029	1.677
Dec	MYD05/MOD05	0.790	1.937	0.459	5.262	-0.579	0.799	2.164	0.482	5.229	-0.850
	Calibrated MYD05/MOD05	0.746	-1.752	0.555	4.845	0.752	0.722	-0.751	0.553	4.588	0.884

All MODIS NIR PWV pixels obtained from both clear and cloudy groups were used.

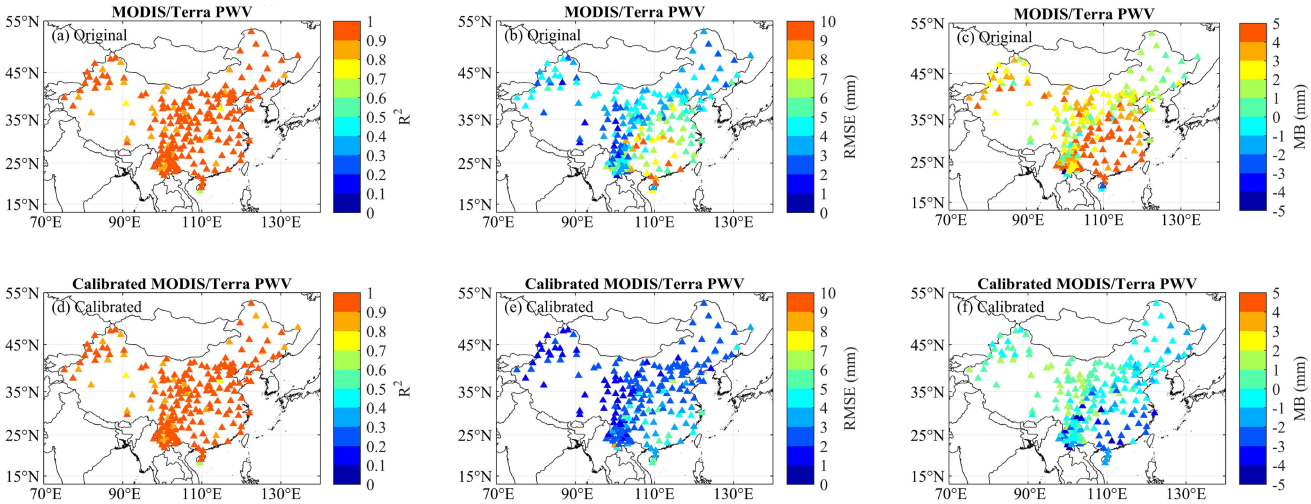

Fig. 18. Annual R^2, RMSE, and MB values for MODIS/Terra PWV measurements against reference GPS PWV measurements at each GPS station from January 1, 2019 to December 31, 2019 over China, using PWV data from the clear group. (a)–(c) Original MODIS/Terra NIR PWV products versus reference GPS-measured PWV data. (d)–(f) Calibrated MODIS/Terra NIR PWV products versus reference GPS-measured PWV data.

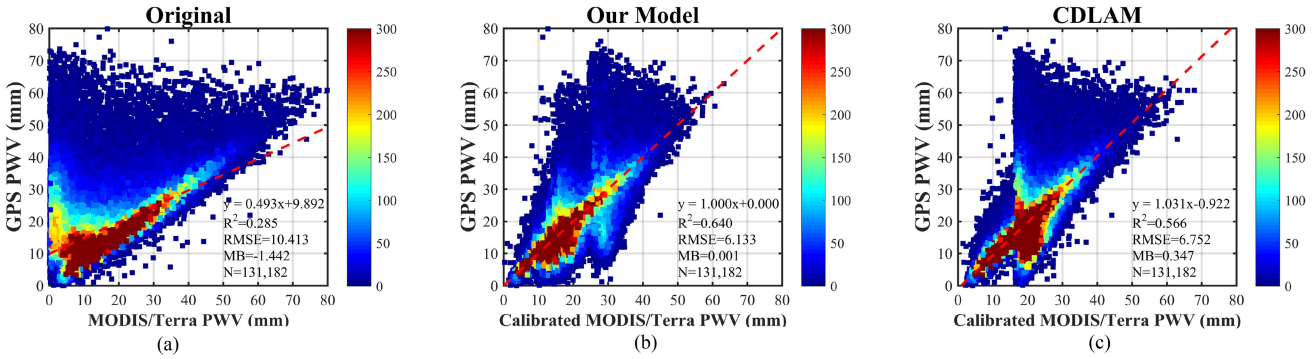

Fig. 19. Evaluation of the PWV data calculated from MODIS/Terra measurements versus the *in situ* GPS-retrieved PWV data from January 1, 2019 to December 31, 2019 over Australia, under all weather conditions. (a) Scatter plots between the official MODIS/Terra NIR PWV products and the ground-based GPS-derived PWV data under all weather conditions. (b) Scatter plots between the calibrated MODIS/Terra NIR PWV products and the ground-based GPS-derived PWV data under all weather conditions, using our model. (c) Scatter plots between the calibrated MODIS/Terra NIR PWV products and the ground-based GPS-derived PWV data under all weather conditions, using CDLAM. Both correction methods are developed and validated using the data of 2019 over Australia. *N* represents the number of spatiotemporally collocated MODIS-GPS data points selected for the comparison analysis. The dashed red lines represent the linear regression results of these data. The points colored with a rainbow scale illustrate the frequency of the MODIS NIR PWV values (brown most frequent, blue least frequent).

thoroughly assessed using the dataset observed in a different time and region. Our LinearDP model utilized GPS PWV as the reference PWV to calibrate the MODIS NIR PWV products, which is different from the previous differential PWV based calibration models that used ECMWF PWV data [57], [58]. In contrast to the previous differential PWV based calibration approaches utilized for the satellite-based IR PWV products [57], [58], our calibration approach was developed for the MODIS NIR PWV products, which is more challenging due to the larger effect of clouds. In addition, we calibrated the MODIS NIR PWV products more frequently (monthly) to enhance the performance of the calibration. This work is the first time to enhance the quality of the official MODIS NIR PWV products under all-weather conditions.

Intercomparison result showed our LinearDP model has slightly better performance in improving the quality of MODIS NIR PWV products in all-weather conditions, as the results presented in Fig. 19. This may be because our Linear approach is developed based on *in situ* high-accuracy GPS PWV data, and this model coefficients are estimated more frequently, namely monthly. In addition, compared with the independent validation result of our model displayed in Fig. 5, our method also showed slightly better accuracy in terms of RMSE, with an RMSE of 6.318 mm smaller than the CDLAM model (RMSE = 6.752 mm). More importantly, our method is calibrated using real world PWV observation data (e.g., GPS). This is different from some other methods (e.g., [57], [58]), where the remote sensing satellite PWV data are calibrated using modeled PWV. The advantage of using real world PWV data in calibration is that 1) it can better reflect PWV variation in the real world; 2) the real PWV observations usually have higher accuracy. The calibration calculation can be done at a more frequent interval (e.g., monthly, seasonally) according to the real world PWV variation.

It is noted that after the performance of our LinearDP model under cloudy condition can still be enhanced, particularly when the PWV values are in the 0–10 mm. The small PWV values do not necessarily suggest the dry atmosphere . This is mainly because satellite-based NIR observations cannot penetrate the clouds in the presence of clouds. Due to the effect of clouds on MODIS NIR PWV retrievals, the official MODIS NIR PWV products cannot provide good quality water vapor measurements in the presence of clouds [54]. The poor quality MODIS NIR PWV products under cloudy conditions resulted in a large variation in the magnitude of differential PWV (ΔPWV) data, in the range of -60 to 20 mm, as shown in Fig. 2(b) and (d). Thus, the regression parameters a and b have a large uncertainty when they are estimated using the poor quality differential PWV under cloudy condition. The calibrated PWV data calculated using a and b therefore have a poor performance. Particularly, all the small value PWV data (0–10 mm) became larger than 10 mm after the calibration. How to calibrate the low PWV values (0–10 mm) accurately still needs to be further investigated in the future.

VI. Conclusion

In this article, we have developed a novel LinearDP calibration model to improve the accuracy of the official MODIS NIR PWV products under both clear and cloudy conditions, using ground-based GPS-derived PWV measurements. The performance of the model was independently validated over both Australia and China using GPS-derived PWV data as references. Our findings from this work can be summarized as follows:

1) Over Australia region, the RMSE for Aqua satellite has reduced by 42.61% for clear group, 41.43% for cloudy group, and 41.45% for MODIS/Aqua both clear and cloudy combined groups. For Terra satellite, the RMSE has reduced by 53.76%, 37.03%, and 39.33% for the clear, cloudy, and combined groups, respectively.
2) Over China region, the RMSE of MODIS/Aqua products was reduced by 31.78%, 24.53%, and 24.93% for the clear, cloudy, and combined groups, respectively. For MODIS/Terra PWV products, the RMSE was reduced

by 38.69%, 28.26%, 28.74% for the clear, cloudy, and combined groups, respectively.

3) The LinearDP model is very robust and stable. Its performance in China is comparable to that in Australia, though the coefficients of the calibration model were estimated using the data from Australia only without data from China.
4) The quality of the water vapor products retrieved from MODIS NIR channels can be significantly improved using this empirical LinearDP regression model. The correlations have been improved and RMSE against ground-based GPS PWV data has been reduced.

Notably, the accuracy of calibrated MODIS NIR PWV products under cloudy sky conditions was still much lower than that under clear sky conditions. It is our future goal to further improve the PWV retrieval accuracy under cloudy conditions.

ACKNOWLEDGMENT

The authors are grateful for MODIS data provided by the National Aeronautics and Space Administration (NASA) Level-1 and Atmosphere Archive and Distribution System (LAADS) Distributed Active Archive Center (DAAC). The authors also gratefully acknowledge the support by the Geoscience Australia, the Crustal Movement Observation Network of China (CMONOC), and the European Centre for Medium-Range Weather Forecasts (ECMWF) for providing their data. The calibrated MODIS water vapor data can be requested from the authors. The calibrated MODIS water vapor data can be requested from the authors.

REFERENCES

[1] T. F. Stocker and Intergovernmental Panel on Climate Change, Eds., *Climate Change 2013: The physical Science Basis ; Summary for Policymakers, a Report of Working Group I of the IPCC, Technical Summary, a Report Accepted by Working Group I of the IPCC But Not Approved in Detail and Frequently Asked Questions; Part of the Working Group I Contribution to the Fifth Assessment Report of the Intergovernmental Panel on Climate Change*. Geneva, Switzerland: Intergovernmental Panel Climate Change, 2013.

[2] K. P. Czajkowski, S. N. Goward, D. Shirey, and A. Walz, "Thermal remote sensing of near-surface water vapor," *Remote Sens. Environ.*, vol. 79, no. 2, pp. 253–265, Feb. 2002.

[3] B. J. Soden, R. T. Wetherald, G. L. Stenchikov, and A. Robock, "Global cooling after the eruption of Mount Pinatubo: A test of climate feedback by water vapor," *Science*, vol. 296, no. 5568, pp. 727–730, Apr. 2002.

[4] T. Schneider, P. A. O'Gorman, and X. J. Levine, "Water vapor and the dynamics of climate changes," *Rev. Geophys.*, vol. 48, no. 3, 2010.

[5] R. Colman, "A comparison of climate feedbacks in general circulation models," *Climate Dyn.*, vol. 20, no. 7, pp. 865–873, May 2003.

[6] G. Myhre et al., "Anthropogenic and natural radiative forcing," in *Proc. Climate Change Phys. Sci. Basis Contribution Work. Group 5th Assessment Rep. Intergovernmental Panel Climate Change*, 2013, pp. 659–740.

[7] H. Ye et al., "Impact of increased water vapor on precipitation efficiency over northern Eurasia," *Geophys. Res. Lett.*, vol. 41, no. 8, pp. 2941–2947, Apr. 2014.

[8] S. W. Seemann, J. Li, W. P. Menzel, and L. E. Gumley, "Operational retrieval of atmospheric temperature, moisture, and ozone from MODIS infrared radiances," *J. Appl. Meteorol. Climatol.*, vol. 42, no. 8, pp. 1072–1091, Aug. 2003.

[9] I. M. Held and B. J. Soden, "Water vapor feedback and global warming," *Annu. Rev. Energy Environ.*, vol. 25, no. 1, pp. 441–475, 2000.

[10] D. Pérez-Ramírez et al., "Evaluation of AERONET precipitable water vapor versus microwave radiometry, GPS, and radiosondes at ARM sites," *J. Geophys. Res.*, vol. 119, no. 15, pp. 9596–9613, Aug. 2014.

[11] S. C. Sherwood, R. Roca, T. M. Weckwerth, and N. G. Andronova, "Tropospheric water vapor, convection, and climate," *Rev. Geophys.*, vol. 48, no. 2, Apr. 2010.

[12] M. A. Sharifi, M. Azadi, and A. S. Khaniani, "Numerical simulation of rainfall with assimilation of conventional and GPS observations over north of Iran," *Ann. Geophys.*, vol. 59, no. 3, May 2016, Art. no. P0322.

[13] W. Rohm, J. Guzikowski, K. Wilgan, and M. Kryza, "4DVAR assimilation of GNSS zenith path delays and precipitable water into a numerical weather prediction model WRF," *Atmos. Meas. Technol.*, vol. 12, no. 1, pp. 345–361, Jan. 2019.

[14] S. Manandhar, S. Dev, Y. H. Lee, Y. S. Meng, and S. Winkler, "A data-driven approach for accurate rainfall prediction," *IEEE Trans. Geosci. Remote Sens.*, vol. 57, no. 11, pp. 9323–9331, Nov. 2019.

[15] Z. Xiong, J. Sang, X. Sun, B. Zhang, and J. Li, "Comparisons of performance using data assimilation and data fusion approaches in acquiring precipitable water vapor: A case study of a western United States of America area," *Water*, vol. 12, no. 10, Oct. 2020, Art. no. 2943.

[16] A. S. Khaniani, H. Motieyan, and A. Mohammadi, "Rainfall forecast based on GPS PWV together with meteorological parameters using neural network models," *J. Atmos. Sol.-Terr. Phys.*, vol. 214, Mar. 2021, Art. no. 105533.

[17] C. Ichoku et al.et al., "Analysis of the performance characteristics of the five-channel microtops II Sun photometer for measuring aerosol optical thickness and precipitable water vapor," *J. Geophys. Res. Atmos.*, vol. 107, no. D13, pp. AAC–AA5, Jul. 2002.

[18] M. D. King, Y. J. Kaufman, W. P. Menzel, and D. Tanré, "Remote sensing of cloud, aerosol, and water vapor properties from the moderate resolution imaging spectrometer (MODIS)," *IEEE Trans. Geosci. Remote Sens.*, vol. 30, no. 1, pp. 2–27, Jan. 1992.

[19] K. E. Trenberth, J. Fasullo, and L. Smith, "Trends and variability in column-integrated atmospheric water vapor," *Climate Dyn.*, vol. 24, no. 7/8, pp. 741–758, Jun. 2005.

[20] Z. Li, J.-P. Muller, and P. Cross, "Comparison of precipitable water vapor derived from radiosonde, GPS, and moderate-resolution imaging spectroradiometer measurements," *J. Geophys. Res. Atmos.*, vol. 108, no. 20, Oct. 2003.

[21] Z. Liu, M. S. Wong, J. Nichol, and P. W. Chan, "A multi-sensor study of water vapour from radiosonde, MODIS and AERONET: A case study of Hong Kong," *Int. J. Climatol.*, vol. 33, no. 1, pp. 109–120, Jan. 2013.

[22] B. J. Soden, D. D. Turner, B. M. Lesht, and L. M. Miloshevich, "An analysis of satellite, radiosonde, and lidar observations of upper tropospheric water vapor from the atmospheric radiation measurement program," *J. Geophys. Res.-Atmos.*, vol. 109, no. D4, Feb. 2004, Art. no. D04105.

[23] O. T. Davies and P. A. Watson, "Comparison of integrated precipitable water vapour obtained by GPS and radiosondes," *Electron. Lett.*, vol. 34, no. 7, pp. 645–646, Apr. 1998.

[24] J. Braun, C. Rocken, and R. Ware, "Validation of line-of-sight water vapor measurements with GPS," *Radio Sci.*, vol. 36, no. 3, pp. 459–472, Jun. 2001.

[25] T. R. Emardson, J. Johansson, and G. Elgered, "The systematic behavior of water vapor estimates using four years of GPS observations," *IEEE Trans. Geosci. Remote Sens.*, vol. 38, no. 1, pp. 324–329, Jan. 2000.

[26] C. Rocken, T. Van Hove, and R. Ware, "Near real-time GPS sensing of atmospheric water vapor," *Geophys. Res. Lett.*, vol. 24, no. 24, pp. 3221–3224, Dec. 1997.

[27] M. P. McCarthy, P. W. Thorne, and H. A. Titchner, "An analysis of tropospheric humidity trends from radiosondes," *J. Climate*, vol. 22, no. 22, pp. 5820–5838, Nov. 2009.

[28] R. J. Ross and W. P. Elliot, "Radiosonde-based Northern Hemisphere tropospheric water vapor trends," *J. Climate*, vol. 14, no. 7, pp. 1602–1612, 2001.

[29] J. Vaquero-Martínez et al.et al., "Validation of MODIS integrated water vapor product against reference GPS data at the Iberian Peninsula," *Int. J. Appl. Earth Observ. Geoinf.*, vol. 63, pp. 214–221, Dec. 2017.

[30] A. S. Khaniani, Z. Nikraftar, and S. Zakeri, "Evaluation of MODIS Near-IR water vapor product over Iran using ground-based GPS measurements," *Atmos. Res.*, vol. 231, Jan. 2020, Art. no. 104657.

[31] S. Mertikas, P. Partsinevelos, A. Tripolitsiotis, C. Kokolakis, G. Petrakis, and X. Frantzis, "Validation of sentinel-3 OLCI integrated water vapor products using regional GNSS measurements in Crete, Greece," *Remote Sens.*, vol. 12, no. 16, Jan. 2020, Art. no. 16.

[32] J. Vaquero-Martínez et al., "Inter-comparison of integrated water vapor from satellite instruments using reference GPS data at the Iberian Peninsula," *Remote Sens. Environ.*, vol. 204, pp. 729–740, Jan. 2018.

[33] Y. Wang et al., "Evaluation of precipitable water vapor from four satellite products and four reanalysis datasets against GPS measurements on the Southern Tibetan Plateau," *J. Climate*, vol. 30, no. 15, pp. 5699–5713, Aug. 2017.

[34] J. Roman, R. Knuteson, T. August, T. Hultberg, S. Ackerman, and H. Revercomb, "A global assessment of NASA AIRS v6 and EUMETSAT IASI v6 precipitable water vapor using ground-based GPS Suominet stations," *J. Geophys. Res.-Atmos.*, vol. 121, no. 15, pp. 8925–8948, Aug. 2016.

[35] J. Xu and Z. Liu, "The first validation of sentinel-3 OLCI integrated water vapor products using reference GPS data in Mainland China," *IEEE Trans. Geosci. Remote Sens.*, vol. 60, 2022, Art. no. 4102817.

[36] H. Wang, X. Liu, K. Chance, G. González Abad, and C. Chan Miller, "Water vapor retrieval from OMI visible spectra," *Atmos. Meas. Tech.*, vol. 7, no. 6, pp. 1901–1913, 2014.

[37] R. Bennartz and J. Fischer, "Retrieval of columnar water vapour over land from backscattered solar radiation using the medium resolution imaging spectrometer," *Remote Sens. Environ.*, vol. 78, no. 3, pp. 274–283, Dec. 2001.

[38] Y. J. Kaufman and B.-C. Gao, "Remote sensing of water vapor in the near IR from EOS/MODIS," *IEEE Trans. Geosci. Remote Sens.*, vol. 30, no. 5, pp. 871–884, Sep. 1992.

[39] J. Xu and Z. Liu, "Radiance-based retrieval of total water vapor content from sentinel-3A OLCI NIR channels using ground-based GPS measurements," *Int. J. Appl. Earth Observ. Geoinf.*, vol. 104, Dec. 2021, Art. no. 102586.

[40] J. Feng and Y. Huang, "Cloud-assisted retrieval of lower-stratospheric water vapor from nadir-view satellite measurements," *J. Atmos. Ocean. Technol.*, vol. 35, no. 3, pp. 541–553, Mar. 2018.

[41] J. Susskind, C. D. Barnet, and J. M. Blaisdell, "Retrieval of atmospheric and surface parameters from AIRS/AMSU/HSB data in the presence of clouds," *IEEE Trans. Geosci. Remote Sens.*, vol. 41, no. 2, pp. 390–409, Feb. 2003.

[42] H. Liu et al., "A physical algorithm for precipitable water vapour retrieval over land using passive microwave observations," *Int. J. Remote Sens.*, vol. 41, no. 16, pp. 6288–6306, Aug. 2020.

[43] D. D. Turner, S. A. Clough, J. C. Liljegren, E. E. Clothiaux, K. E. Cady-Pereira, and K. L. Gaustad, "Retrieving liquid water path and precipitable water vapor from the atmospheric radiation measurement (ARM) microwave radiometers," *IEEE Trans. Geosci. Remote Sens.*, vol. 45, no. 11, pp. 3680–3690, Nov. 2007.

[44] D. P. Dee et al., "The ERA-interim reanalysis: Configuration and performance of the data assimilation system," *Quart. J. Roy. Meteorol. Soc.*, vol. 137, no. 656, pp. 553–597, Apr. 2011.

[45] S. M. Uppala et al., "The ERA-40 re-analysis," *Quart. J. Roy. Meteorol. Soc.*, vol. 131, no. 612, pp. 2961–3012, Oct. 2005.

[46] S. Kobayashi et al., "The JRA-55 reanalysis: General specifications and basic characteristics," *J. Meteorol. Soc. Jpn.*, vol. 93, no. 1, pp. 5–48, 2015.

[47] A. Ebita et al., "The Japanese 55-year reanalysis 'JRA-55': An interim report," *Sola*, vol. 7, pp. 149–152, 2011.

[48] G. Fu, S. P. Charles, B. Timbal, B. Jovanovic, and F. Ouyang, "Comparison of NCEP-NCAR and ERA-interim over Australia," *Int. J. Climatol.*, vol. 36, no. 5, pp. 2345–2367, Apr. 2016.

[49] E. Kalnay et al., "The NCEP/NCAR 40-year reanalysis project," *Bull. Amer. Meteorol. Soc.*, vol. 77, no. 3, pp. 437–471, Mar. 1996.

[50] Q. Zhang, J. Ye, S. Zhang, and F. Han, "Precipitable water vapor retrieval and analysis by multiple data sources: Ground-based GNSS, radio occultation, radiosonde, microwave satellite, and NWP reanalysis data," *J. Sens.*, vol. 2018, 2018, Art. no. 3428303.

[51] H. Hu, R. Yang, W.-C. Lee, Y. Cao, J. Mao, and L. Gao, "Multi-sensor study of precipitable water vapor and atmospheric profiling from microwave radiometer, GNSS/MET, radiosonde, and ECMWF reanalysis in Beijing," *J. Appl. Remote Sens.*, vol. 14, no. 4, Dec. 2020, Art. no. 044514.

[52] B.-C. Gao and Y. J. Kaufman, "Water vapor retrievals using moderate resolution imaging spectroradiometer (MODIS) near-infrared channels," *J. Geophys. Res. Atmos.*, vol. 108, no. D13, 2003.

[53] V. V. Salomonson, W. L. Barnes, P. W. Maymon, H. E. Montgomery, and H. Ostrow, "MODIS: Advanced facility instrument for studies of the Earth as a system," *IEEE Trans. Geosci. Remote Sens.*, vol. 27, no. 2, pp. 145–153, Mar. 1989.

[54] J. He and Z. Liu, "Comparison of satellite-derived precipitable water vapor through near-infrared remote sensing channels," *IEEE Trans. Geosci. Remote Sens.*, vol. 57, no. 12, pp. 10252–10262, Dec. 2019.

[55] J. Bai, Y. Lou, W. Zhang, Y. Zhou, Z. Zhang, and C. Shi, "Assessment and calibration of MODIS precipitable water vapor products based on GPS network over China," *Atmos. Res.*, vol. 254, Jun. 2021, Art. no. 105504.

[56] D. Zhu, K. Zhang, L. Yang, S. Wu, and L. Li, "Evaluation and calibration of MODIS near-infrared precipitable water vapor over China using GNSS observations and ERA-5 reanalysis dataset," *Remote Sens.*, vol. 13, no. 14, Jan. 2021, Art. no. 14.

[57] L. Chang, R. Xiao, A. A. Prasad, G. Gao, G. Feng, and Y. Zhang, "Cloud mask-related differential linear adjustment model for MODIS infrared water vapor product," *Remote Sens. Environ.*, vol. 221, pp. 650–664, Feb. 2019.

[58] L. Chang, Y. Li, Z. Han, G. Feng, Y. Li, and Y. Zhang, "Improvement of precipitable water vapour and water vapour mixing ratio profile in atmospheric infrared sounder retrievals: Differential linear adjustment model," *Int. J. Remote Sens.*, vol. 41, no. 17, pp. 6858–6875, Sep. 2020.

[59] J. He and Z. Liu, "Water vapor retrieval from MERSI NIR channels of fengyun-3B satellite using ground-based GPS data," *Remote Sens. Environ.*, vol. 258, Jun. 2021, Art. no. 112384.

[60] Y. Feng and S. Du, "Climate changes and landscape responses of China during the past 40 years (1979–2018) under Köppen–Geiger climate classification," *ISPRS Ann. Photogrammetry, Remote Sens. Spatial Inf. Sci.*, vol. 3, pp. 731–737, 2020.

[61] C. Pigram, "Geoscience Australia—A multi disciplined agency," *Episodes J. Int. Geosci.*, vol. 35, no. 4, pp. 524–525, Dec. 2012.

[62] Q. Chen, S. Song, S. Heise, Y.-A. Liou, W. Zhu, and J. Zhao, "Assessment of ZTD derived from ECMWF/NCEP data with GPS ZTD over China," *GPS Solutions*, vol. 15, no. 4, pp. 415–425, Oct. 2011.

[63] MODIS Science Team, "MOD03 MODIS/Terra geolocation fields 5-Min L1A Swath 1km," *Level 1 Atmos. Arch. Distrib. Syst.*, doi: 10.5067/MODIS/MOD03.006.

[64] MODIS Atmosphere Science Team, "MOD05_L2 MODIS/terra total precipitable water vapor 5-min L2 Swath 1km and 5km," *NASA Level 1 Atmos. Arch. Distrib. Syst.*, 2015, doi: 10.5067/MODIS/MOD05_L2.006.

[65] S. Platnick et al., "The MODIS cloud products: Algorithms and examples from terra," *IEEE Trans. Geosci. Remote Sens.*, vol. 41, no. 2, pp. 459–473, Feb. 2003.

[66] H. Hersbach et al., "The ERA5 global reanalysis," *Quart. J. Roy. Meteorol. Soc.*, vol. 146, no. 730, pp. 1999–2049, Jul. 2020, doi: 10.1002/qj.3803.

[67] L. Hoffmann et al., "From ERA-interim to ERA5: The considerable impact of ECMWF's next-generation reanalysis on Lagrangian transport simulations," *Atmos. Chem. Phys.*, vol. 19, pp. 3097–3124, Mar. 2019.

[68] C. Albergel et al., "ERA-5 and ERA-interim driven ISBA land surface model simulations: Which one performs better?," *Hydrol. Earth Syst. Sci.*, vol. 22, no. 6, pp. 3515–3532, Jun. 2018.

[69] S. Wang et al., "Evaluation of precipitable water vapor from five reanalysis products with ground-based GNSS observations," *Remote Sens.*, vol. 12, no. 11, Jun. 2020, Art. no. 1817.

[70] M. Bevis, S. Businger, T. A. Herring, C. Rocken, R. A. Anthes, and R. H. Ware, "GPS meteorology: Remote sensing of atmospheric water vapor using the global positioning system," *J. Geophys. Res. Atmos.*, vol. 97, no. D14, pp. 15787–15801, Oct. 1992.

[71] X. Wang, K. Zhang, S. Wu, S. Fan, and Y. Cheng, "Water vapor-weighted mean temperature and its impact on the determination of precipitable water vapor and its linear trend," *J. Geophys. Res. Atmos.*, vol. 121, no. 2, pp. 833–852, Jan. 2016.

[72] Y. Yuan, K. Zhang, W. Rohm, S. Choy, R. Norman, and C.-S. Wang, "Real-time retrieval of precipitable water vapor from GPS precise point positioning," *J. Geophys. Res. Atmos.*, vol. 119, no. 16, pp. 10044–10057, Aug. 2014.

[73] R. Keys, "Cubic convolution interpolation for digital image processing," *IEEE Trans. Acoust., Speech, Signal Process.*, vol. 29, no. 6, pp. 1153–1160, Dec. 1981.

[74] J. He and Z. Liu, "Water vapor retrieval from MODIS NIR channels using ground-based GPS data," *IEEE Trans. Geosci. Remote Sens.*, vol. 58, no. 5, pp. 3726–3737, May 2020.

Jiafei Xu received the B.Sc. degree in remote sensing science and technology from Shandong Agricultural University, Tai'an, China, in 2015, and the M.Sc. degree in geomatics engineering from Aerospace Information Research Institute, Chinese Academy of Sciences (CAS), Beijing, China, in 2019. He is currently working the Ph.D. degree with the Department of Land Surveying and Geo-Informatics, The Hong Kong Polytechnic University, Hong Kong, China.

His current research interests include the algorithm development for precipitable water vapor retrieval from multisensor data using ground-based GNSS measurements, and the algorithm validation for various space-sensed precipitable water vapor products by conducting comparisons with reference data, such as GNSS, radiometer, and reanalysis products.

Zhizhao Liu (Member, IEEE) received the B.Sc. degree in surveying engineering from Jiangxi University of Science and Technology, Ganzhou, China, in 1994; the M.Sc. degree in geodesy from the Wuhan University, Wuhan, China, in 1997; and the Ph.D. degree in geomatics engineering from the University of Calgary, Calgary, Alberta, Canada, in 2004.

He is currently a Professor and the Associate Head of the Department of Land Surveying and Geo-Informatics, The Hong Kong Polytechnic University, Kowloon, Hong Kong, China. His research interests include new algorithm development for precise global positioning system (GPS) and global navigation satellite system (GNSS), GPS/GNSS precise point positioning (PPP), ionosphere modeling and scintillation monitoring, tropospheric remote sensing and modeling, and GPS/GNSS meteorology. He has over 20 years of experience in GPS/GNSS research.

Dr. Liu was the recipient of the inaugural Early Career Award of the Hong Kong Research Grants Council (RGC), Hong Kong, in 2012 and was the recipient of the inaugural Best Conference Paper of the China Satellite Navigation Conference (CSNC), China, in 2013. In 2014, he was nominated by the Hong Kong Observatory for the World Meteorological Organization (WMO) "Norbert Gerbier-MUMM International Award for 2015" for his paper that has developed a method to evaluate the absolute accuracy of water vapor measurements, in addition to other numerous awards and honors.